A Presentation to the HFIP Telecon

Satellite Data Assimilation in Regional Models: Promises and Challenges

Xiaolei Zou

Department of Earth, Ocean and Atmospheric Sciences

Florida State University, USA

September 4, 2013

Outline

- Important Building Blocks for Satellite DA
- GOES Imager Radiance Assimilation in GSI/ARW
- POSE MHS Radiance Assimilation in GSI/ARW
- SNPP ATMS Radiance Assimilation in GSI/HWRF
- Summary & Conclusions

Important Building Blocks for Satellite DA

$$J(\mathbf{x}_0) = \frac{1}{2}(\mathbf{x}_0 - \mathbf{x}^b)^T \mathbf{B}^{-1}(\mathbf{x}_0 - \mathbf{x}^b) + \frac{1}{2}(H(\mathbf{x}_0) - \mathbf{y}^{obs})^T (\mathbf{O}+\mathbf{F})^{-1}(H(\mathbf{x}_0) - \mathbf{y}^{obs})$$

$$J(\mathbf{x}^a) = \min_{\mathbf{x}_0} J(\mathbf{x}_0)$$

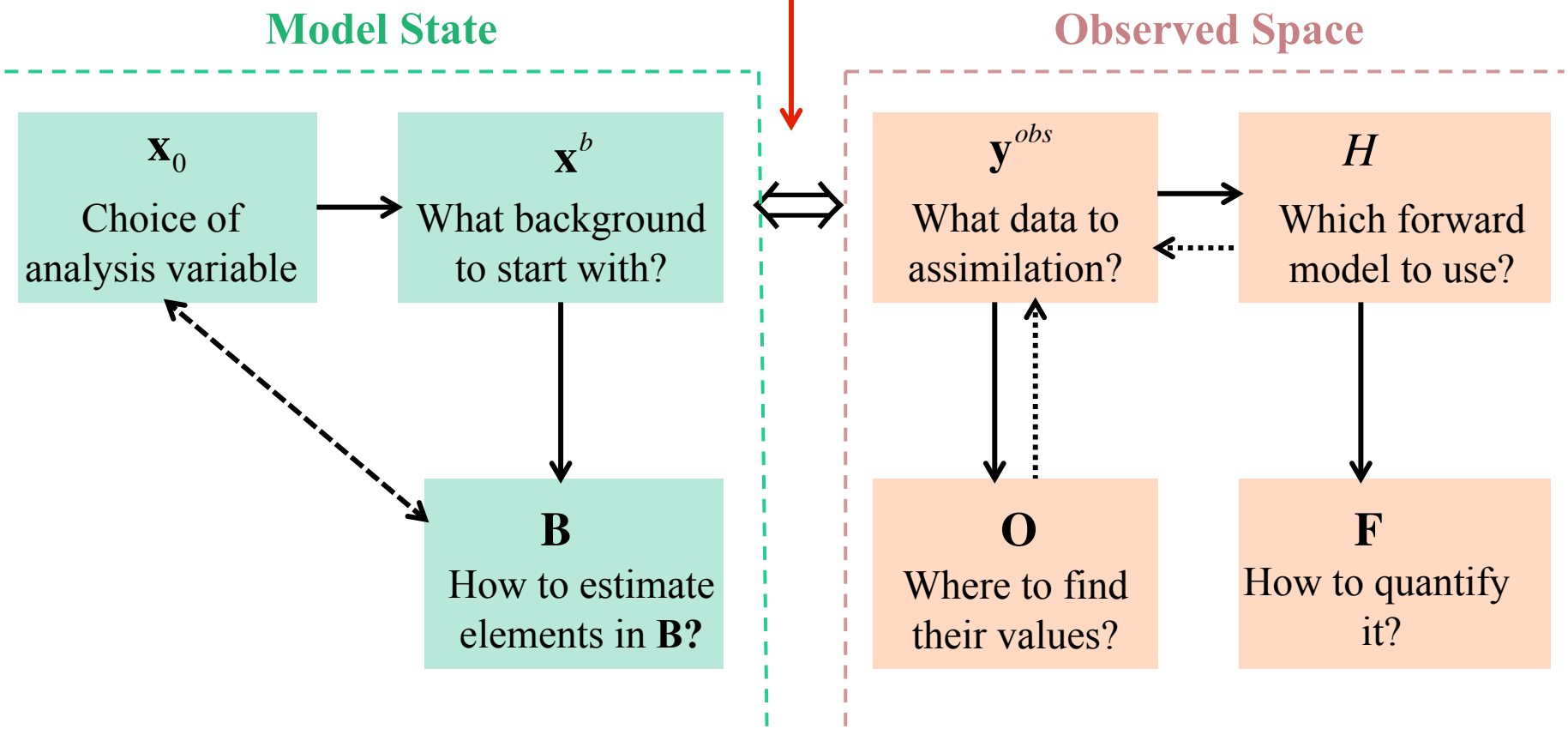

Part I

An Evaluation of Added Benefits of GOES Imager Radiances to Other Satellite Data Assimilation

GOES Imager Radiance Assimilation in GSI/ARW

1) Comparison of Single Type Satellite Data Assimilation

✓ AMSU-A	✓ HIRS/4	✓ HIRS/3	✓ GSN
✓ AIRS	✓ AIRS	✓ MHS	✓ GOES Imager

2) GOES Imager Added to Different Types of Satellite Data

3) GOES Imager Added to All Satellite Data Assimilation

4) Impact of Quality Control on MHS Data Assimilation

GOES West (11) and GOES East (12)

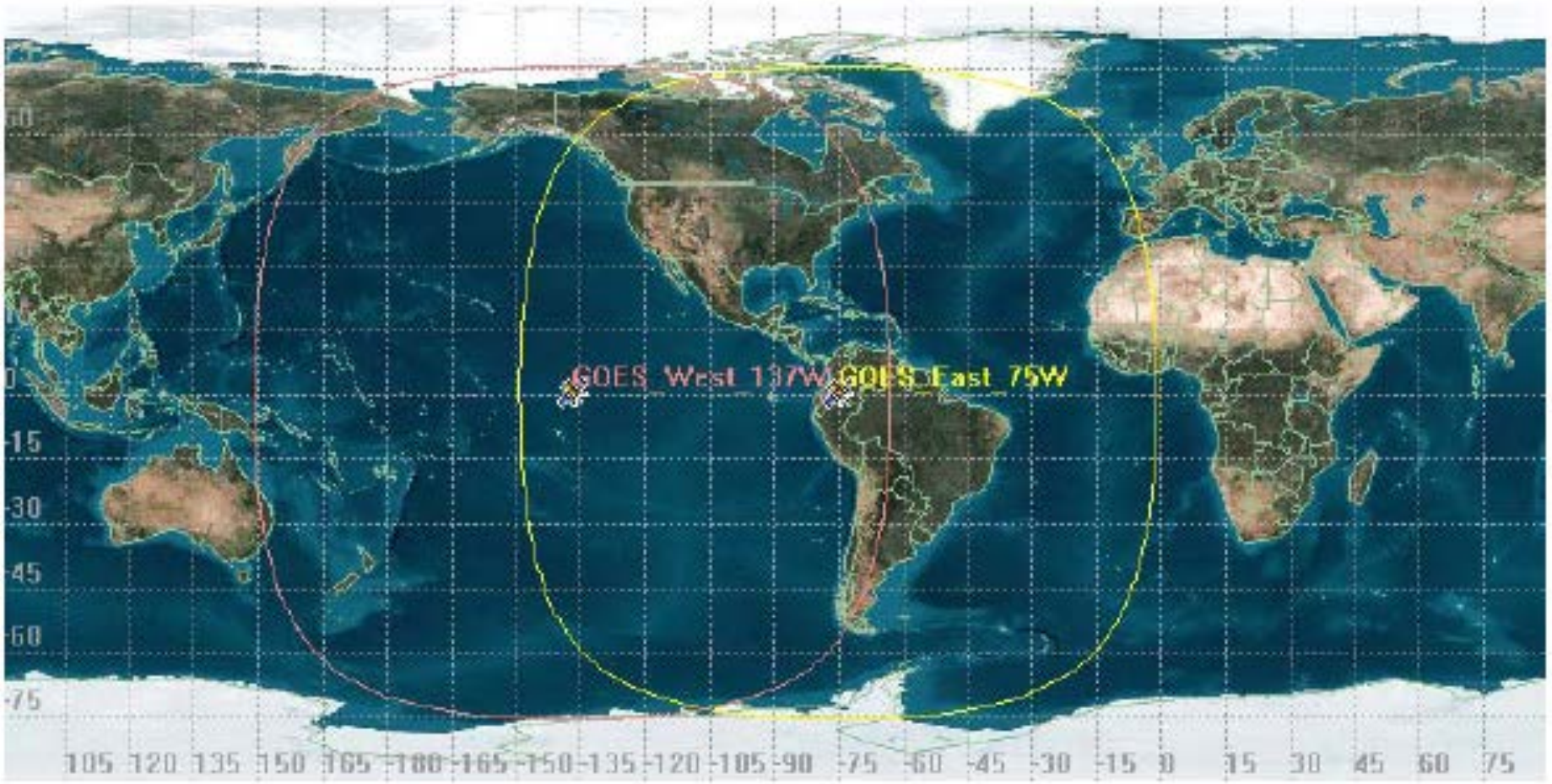

GOES-R Series Imagery Coverage Figure

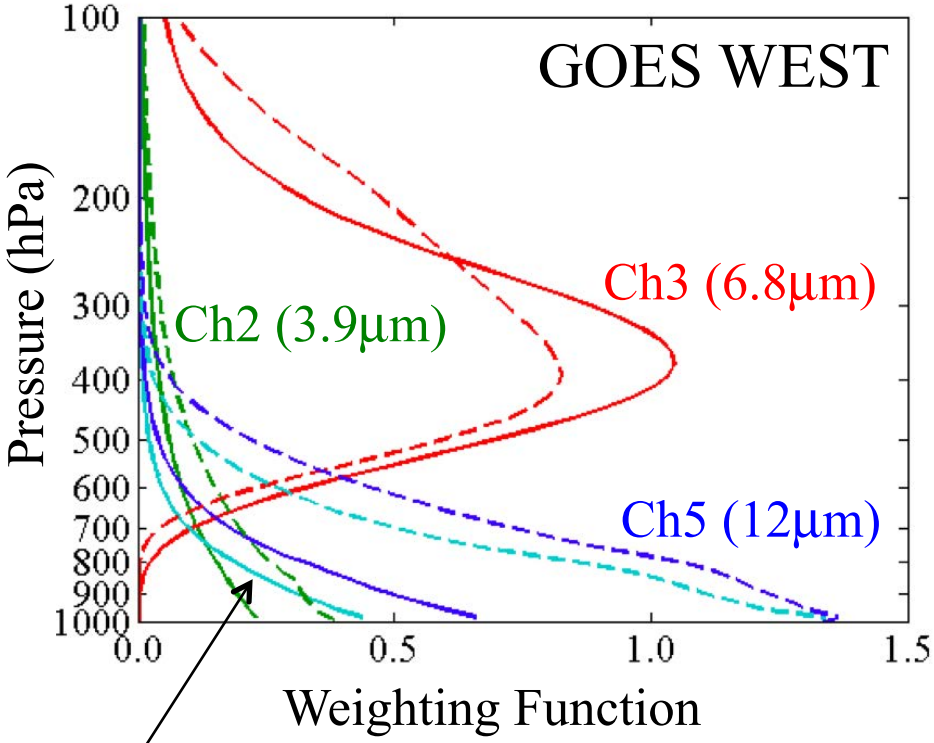

Ch2: near-infrared (low cloud, fog, fire)
Ch3: infrared (upper-level water vapor)
Ch4: infrared (surface and cloud-top T)
Ch5: infrared (low-level water vapor)
Ch6: infrared (cloud detection)

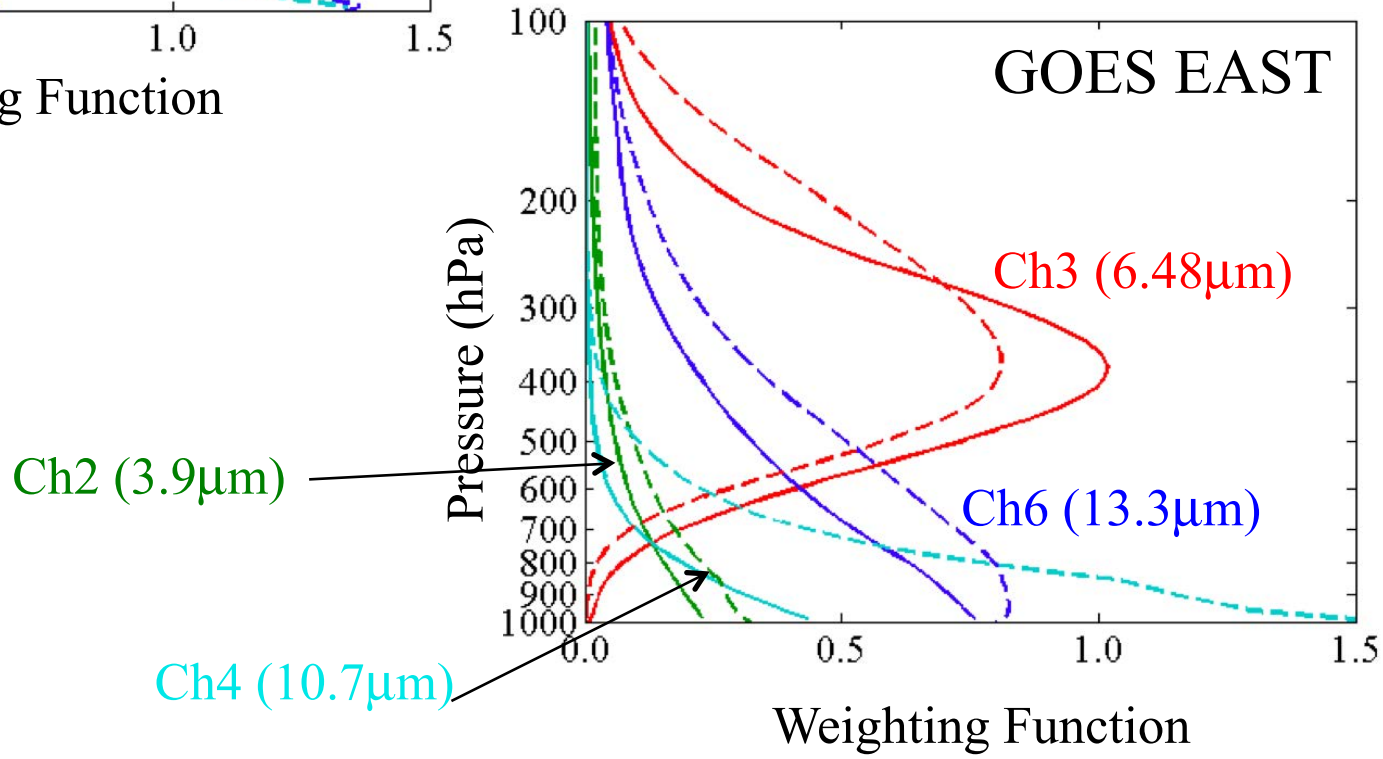

Mean Jacobian of Brightness Temperature

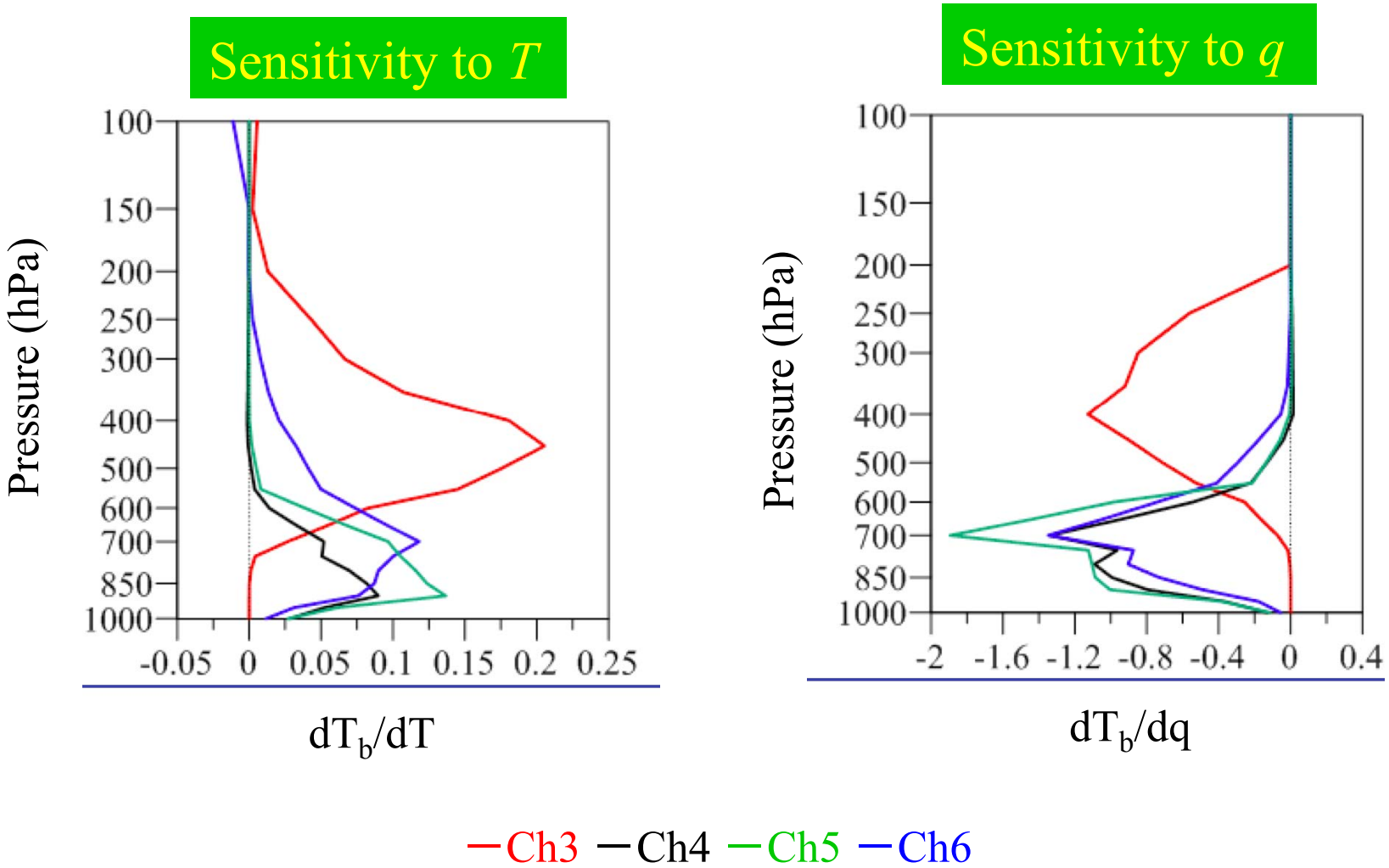

Advanced Research WRF (ARW) Model Domain

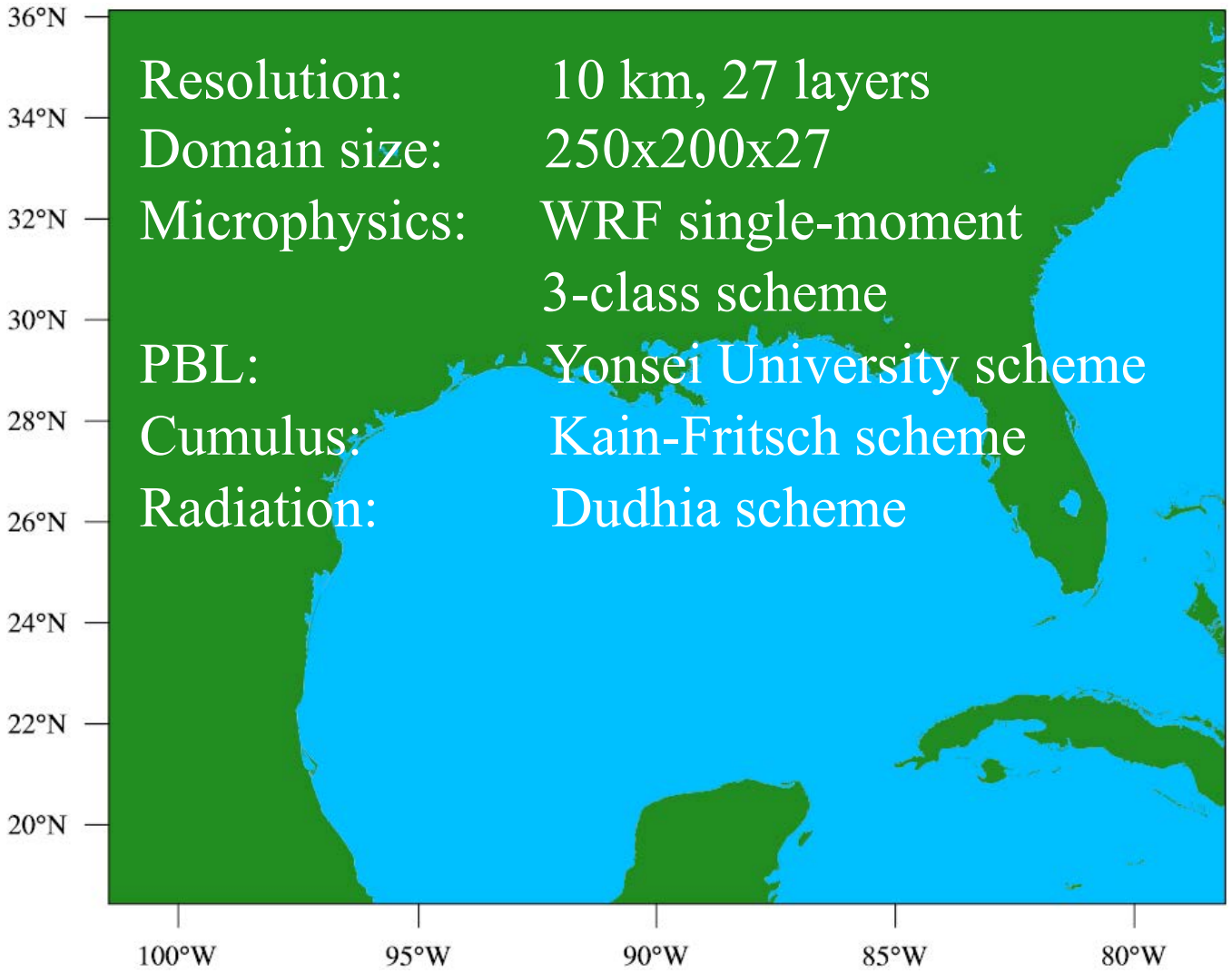

NCEP GSI 3D-Var Data Assimilation System

Assimilation of Different Combinations of Observations

AMSU-A, AIRS, HIRS/3, HIRS/4, MHS, GSN,

GOES imager, Conventional data

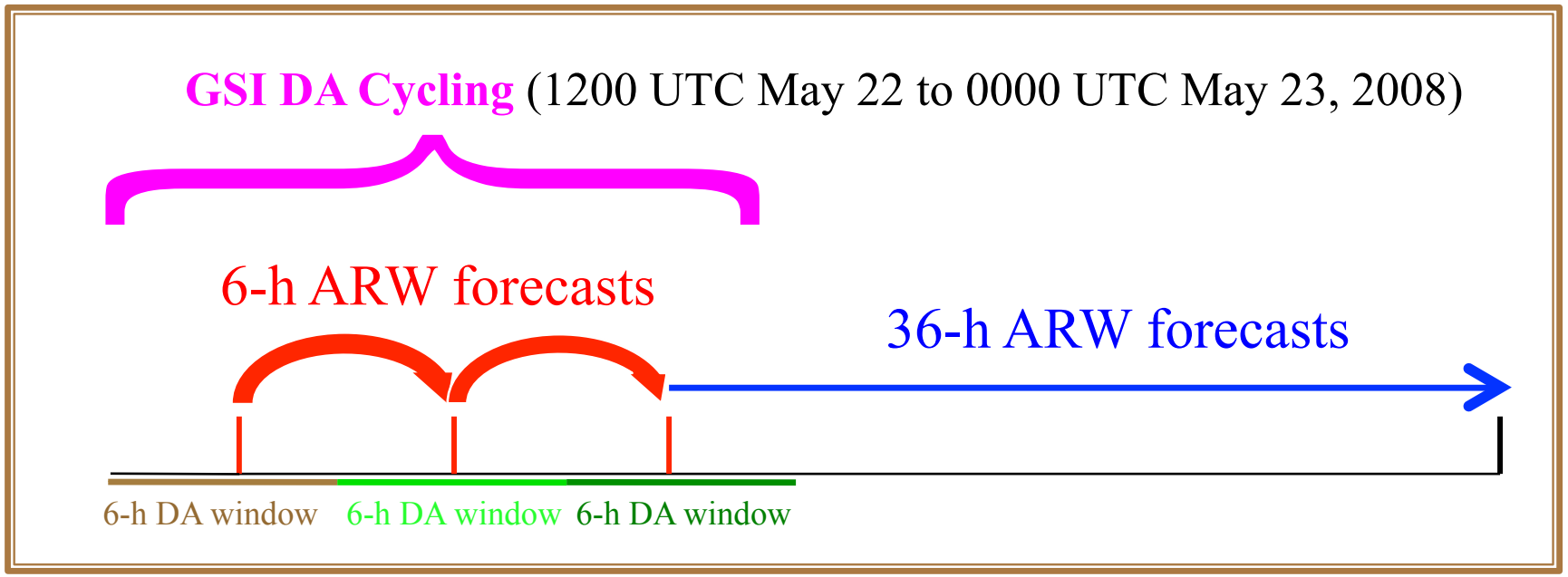

Satellite	Instruments	Satellite	Instruments	Satellite	Instruments
NOAA-14	[HIRS/2][1]	**MetOp-A**	**HIRS/4**	**GOES-11**	(SNDR)
	[MSU]		**AMSU-A**		**Imager**
NOAA-15	**AMSU-A**		**MHS**		**SNDRD1**
	AMSU-B		[IASI]		**SNDRD2**
NOAA-16	(HIRS/3) [2]	**Aqua**	**AIRS**		**SNDRD3**
	(AMSU-A)		(AMSU-A)		**SNDRD4**
	AMSU-B		(AMSRE)	**GOES-12**	(SNDR)
	(AVHRR3)	**F13**	(SSMI)		**Imager**
NOAA-17	**HIRS/3**	**F14**	(SSMI)		**SNDRD1**
	(AMSU-A)	**F15**	(SSMI)		**SNDRD2**
	AMSU-B	**F16**	(SSMIS)		**SNDRD3**
	(AVHRR3)				**SNDRD4**
NOAA-18	(HIRS/4)			**GOES-13**	(SNDR)
	AMSU-A				(Imager)
	MHS				(SNDRD1)
	(AVHRR3)				(SNDRD2)
[1]Data not available for this case.					(SNDRD3)
[2]Instruments removed from operational data assimilation.					(SNDRD4)

Total Data Count

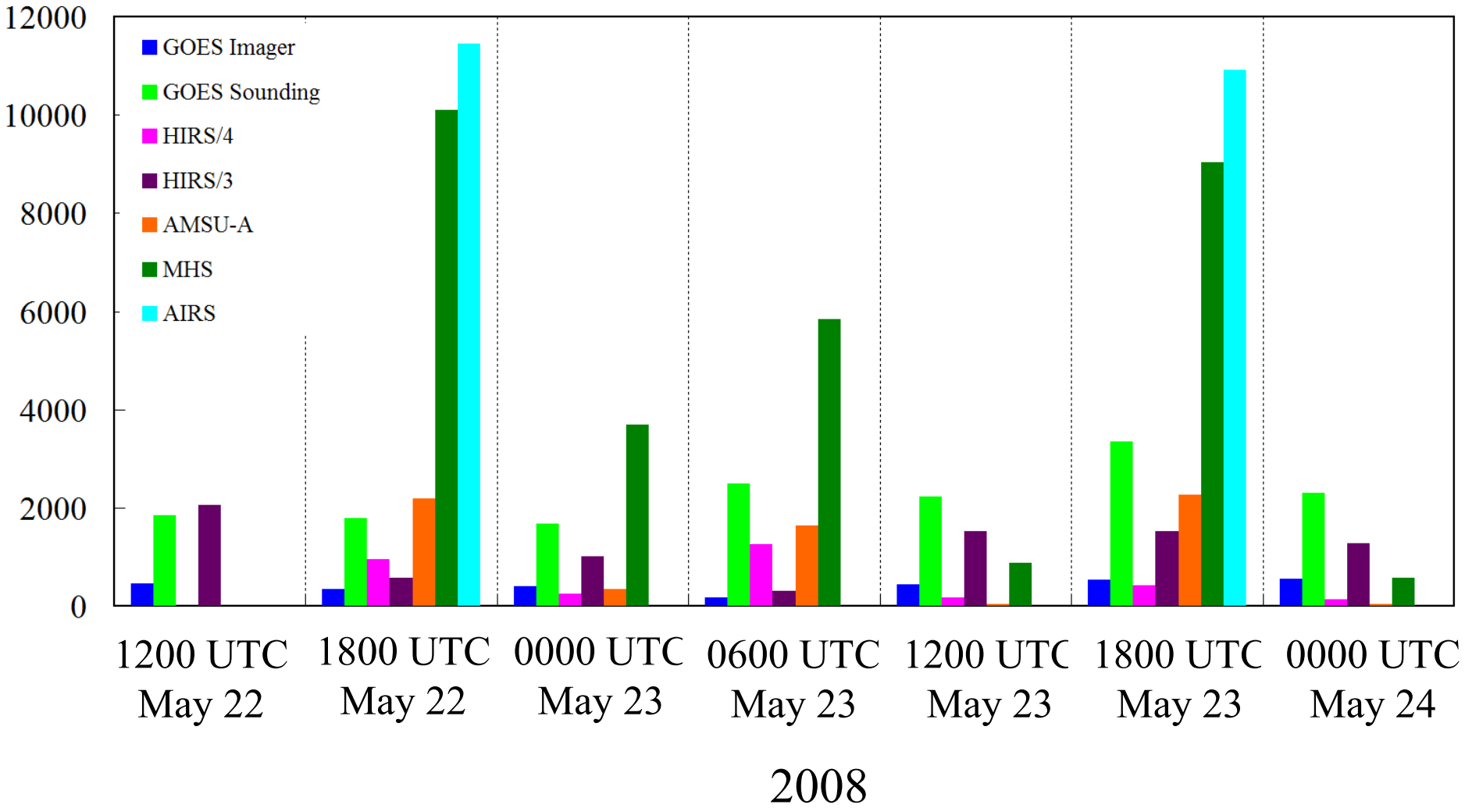

UTC Dependence of POES Data Count

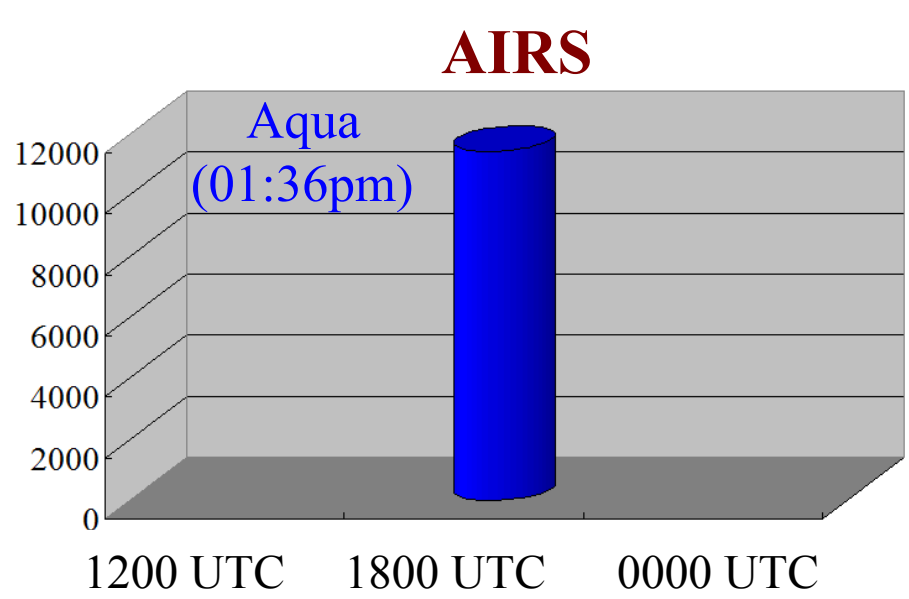

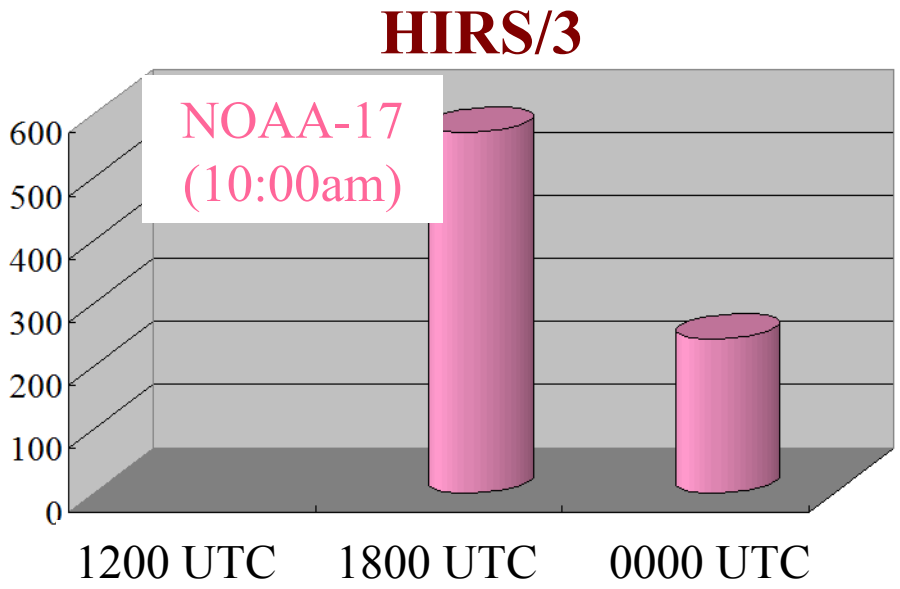

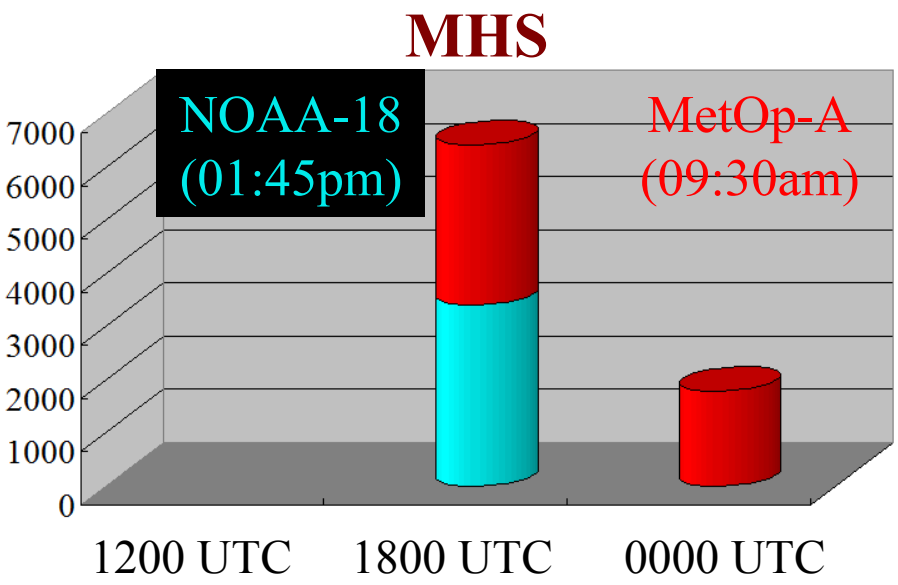

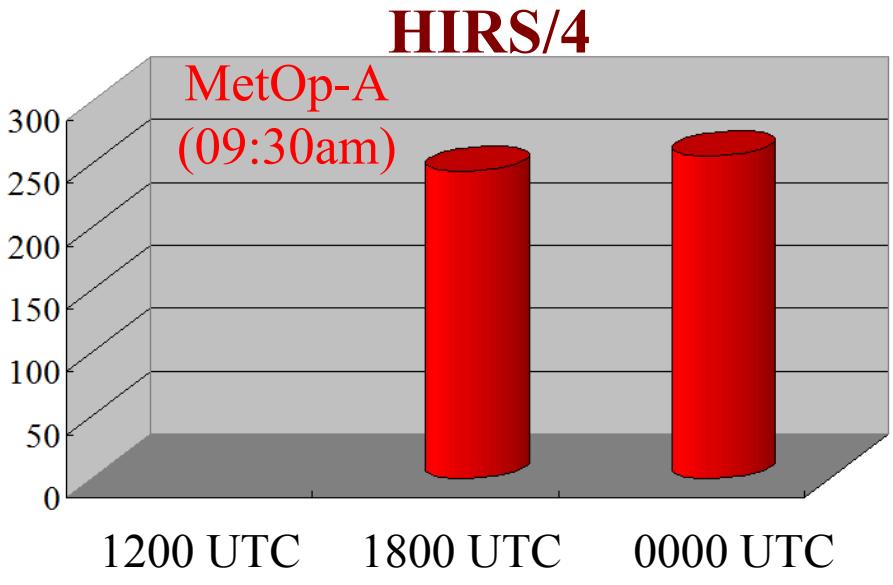

GOES Imager Data Count

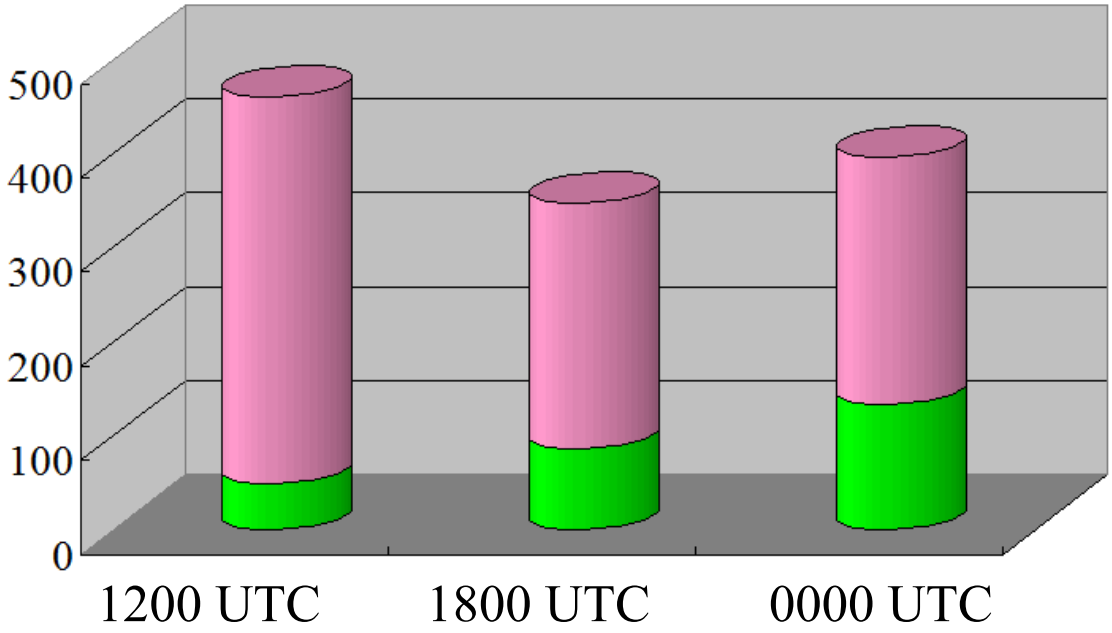

G11-Imager

G12-Imager

O-B for AMSU-A (NOAA-18)

1800 UTC May 22, 2008

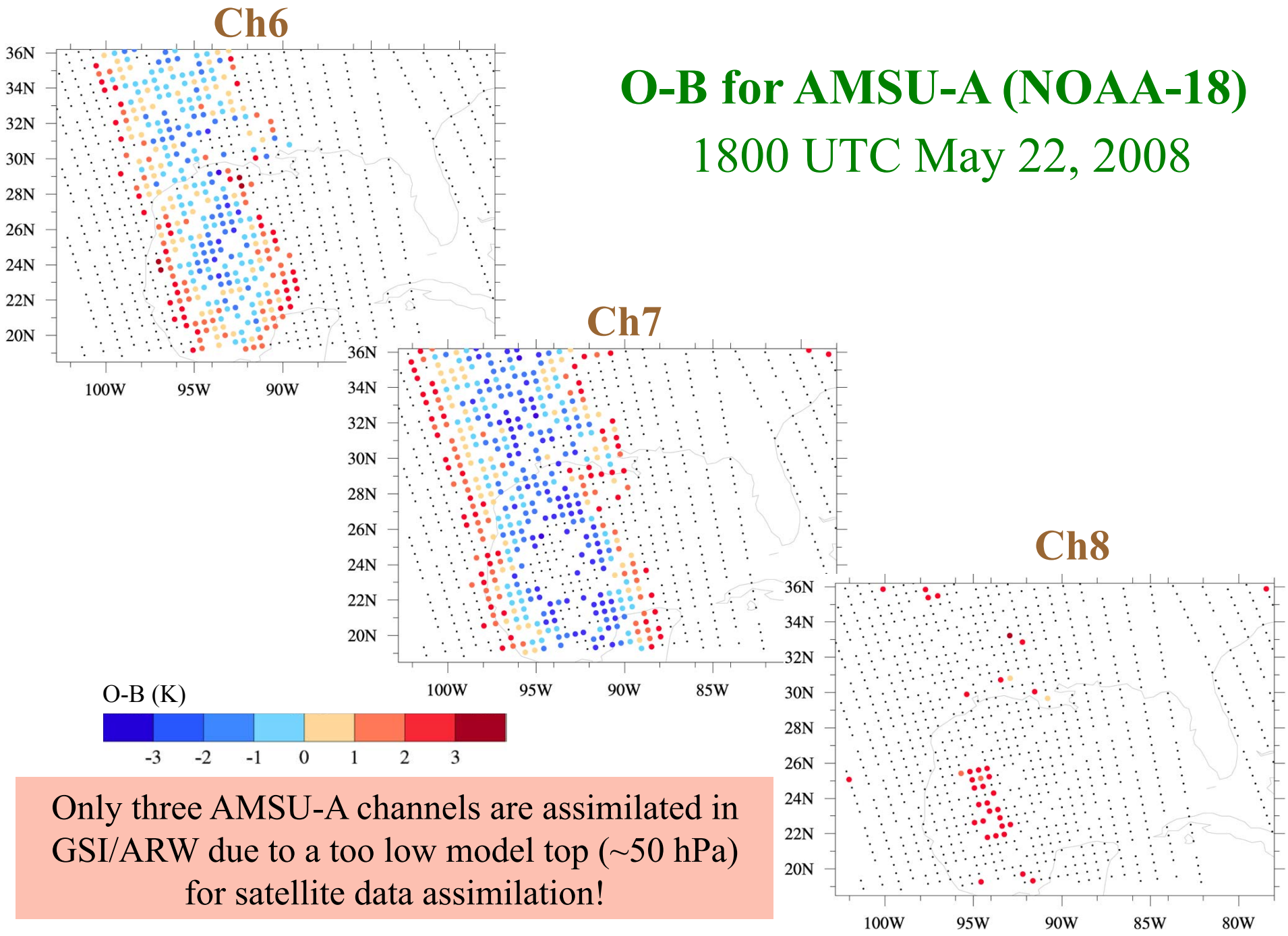

Only three AMSU-A channels are assimilated in GSI/ARW due to a too low model top (~50 hPa) for satellite data assimilation!

Observed BT of GOES-11 Ch5 on May 23, 2008

0300-0306 UTC

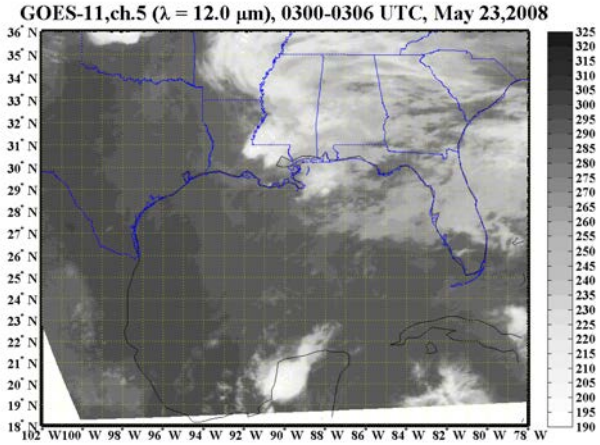

0600-0606 UTC

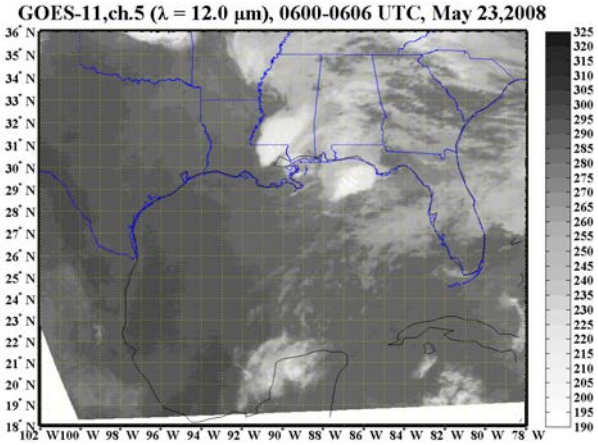

0900-0906 UTC

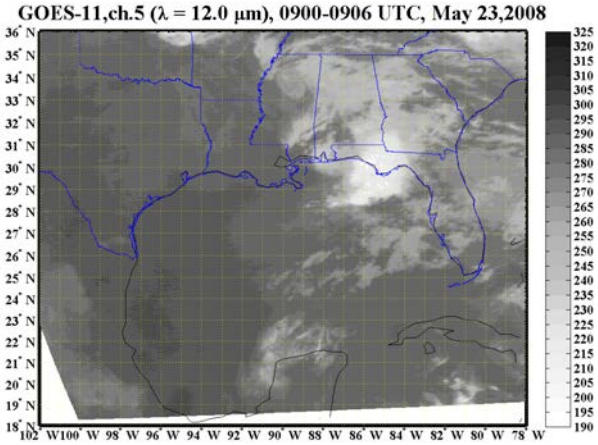

1200-1206 UTC

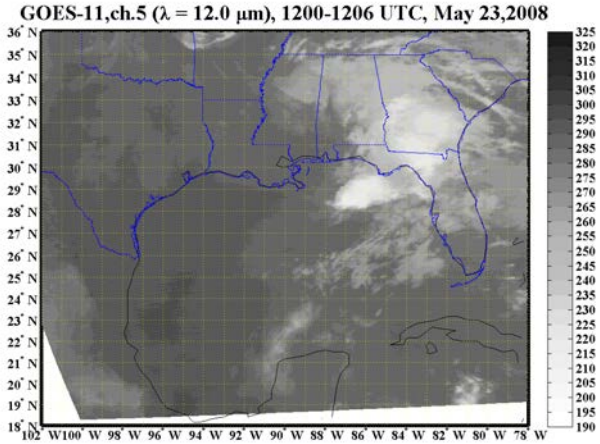

1500-1506 UTC

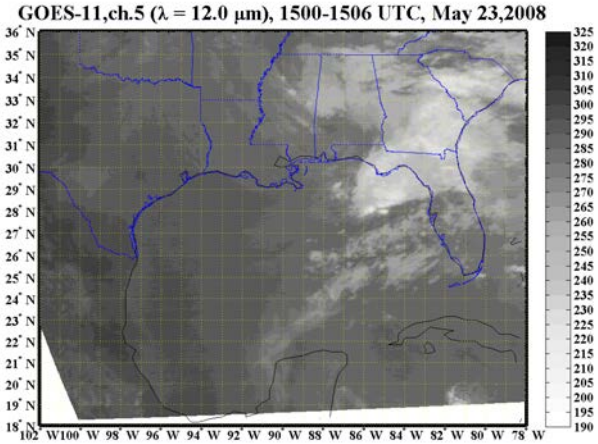

1800-1806 UTC

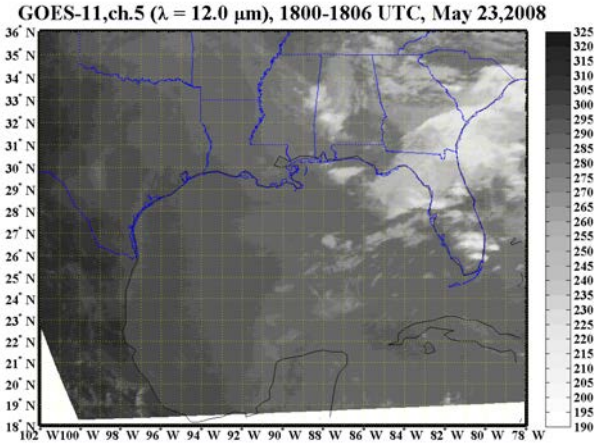

12-h Forecast Differences at 850 hPa

1200 UTC May 23 2008

Mixing Ratio
GOES_Img - CONV

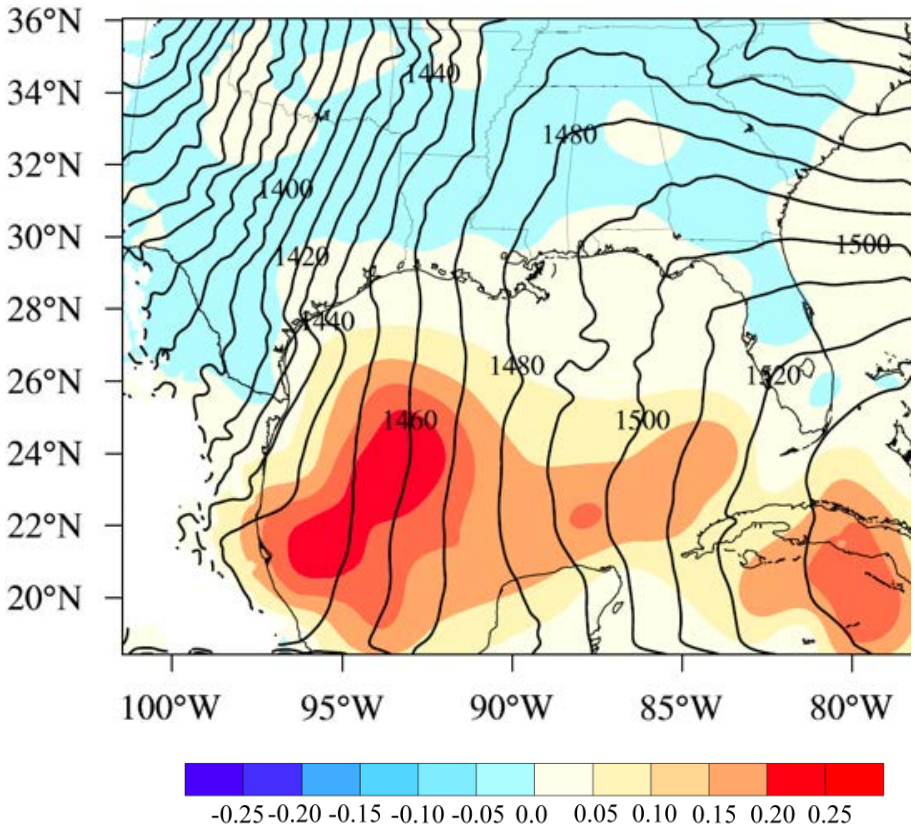

Temperature
GOES_Img - CONV

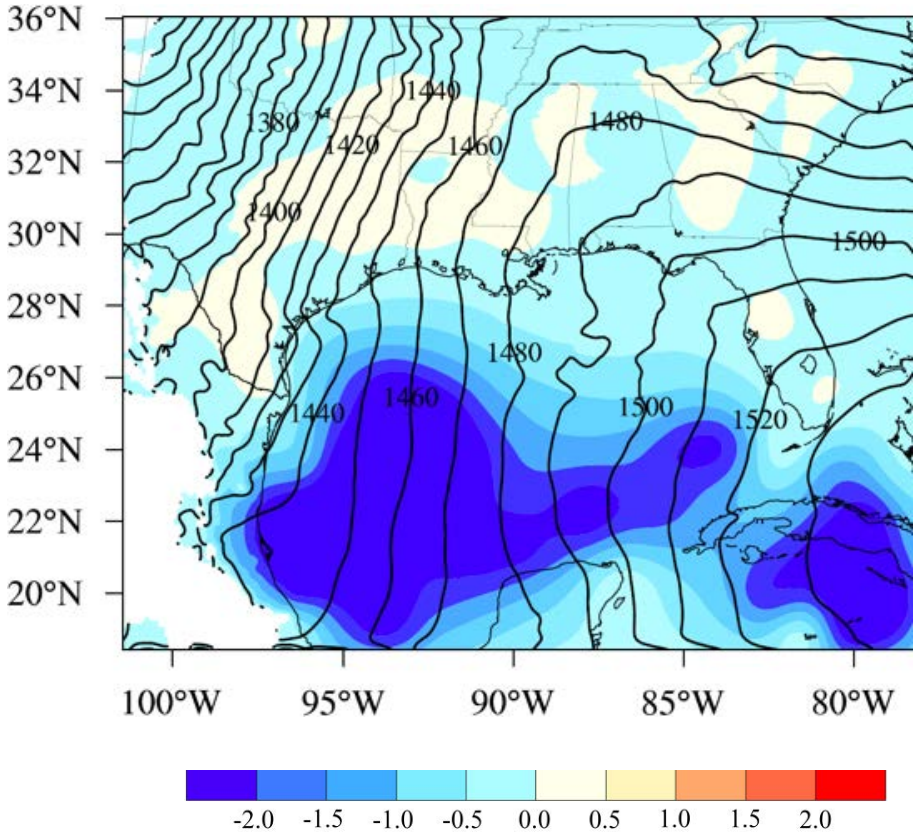

Threat Scores of 3-h Accumulative Rainfall at 1mm thresholds Averaged over 24 Hours

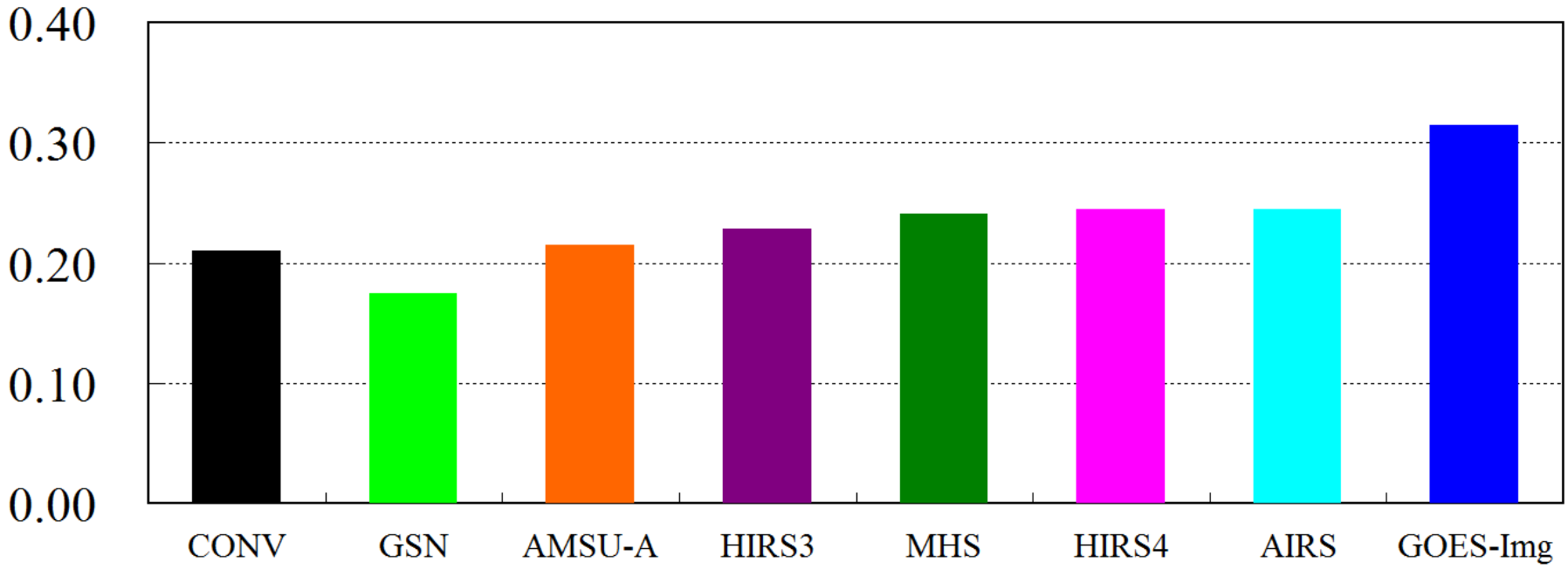

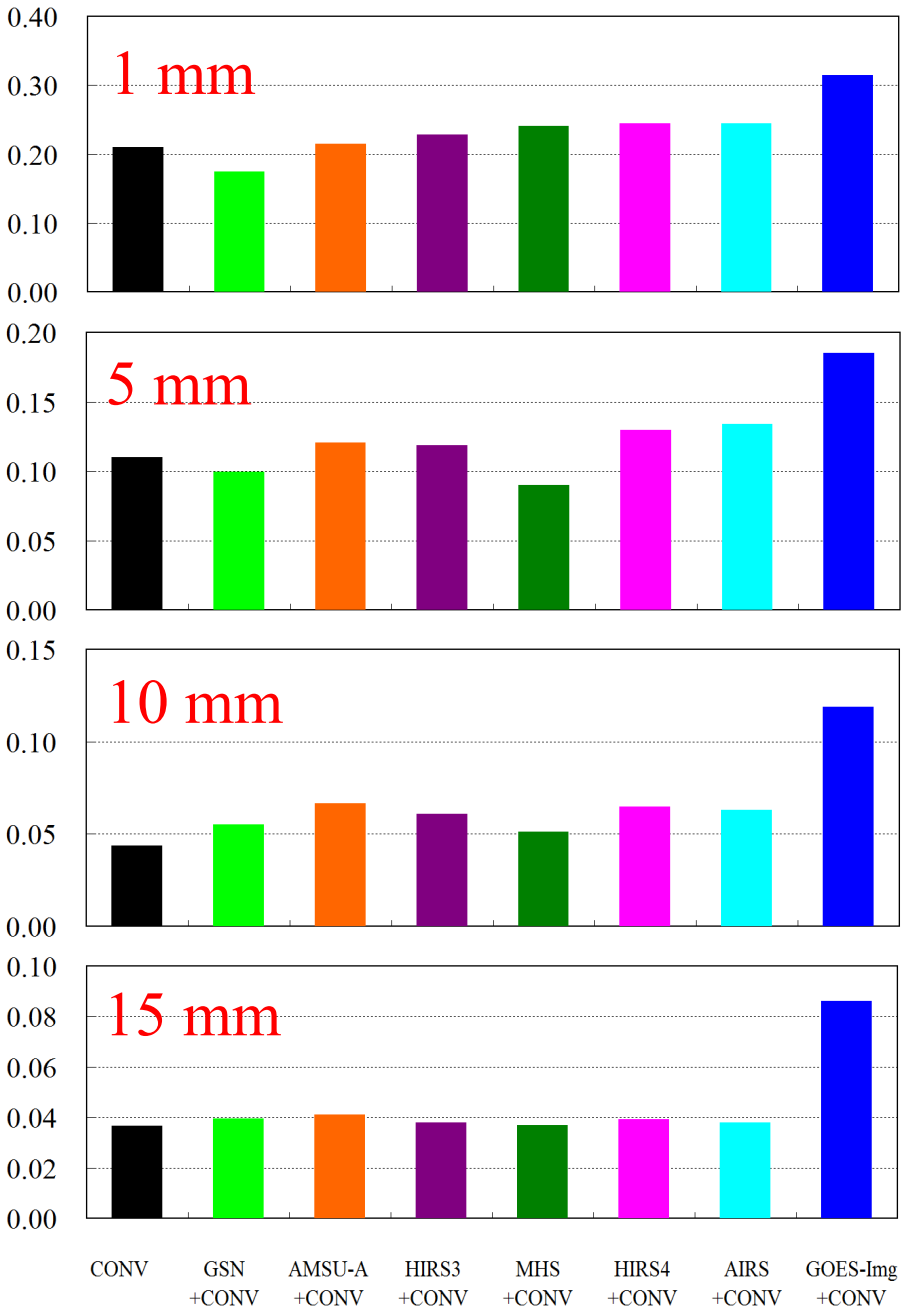

Threat Scores of 3-h Accumulative Rainfall Averaged over 24 Hours

Assimilation of a Single Type of Satellite Observations

Threat Scores of 3-h Accumulative Rainfall at 5mm thresholds Averaged over 24 Hours

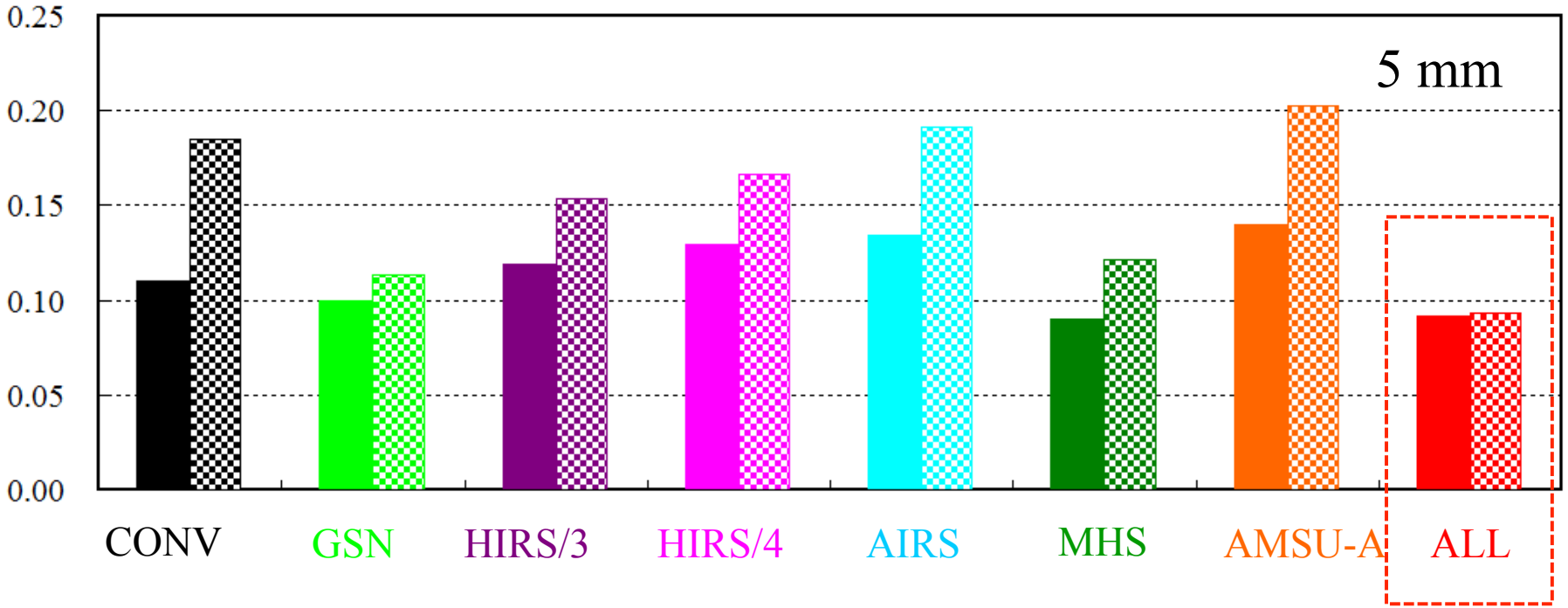

Left bar: without GOES Imager data

Right bar: with GOES Imager data

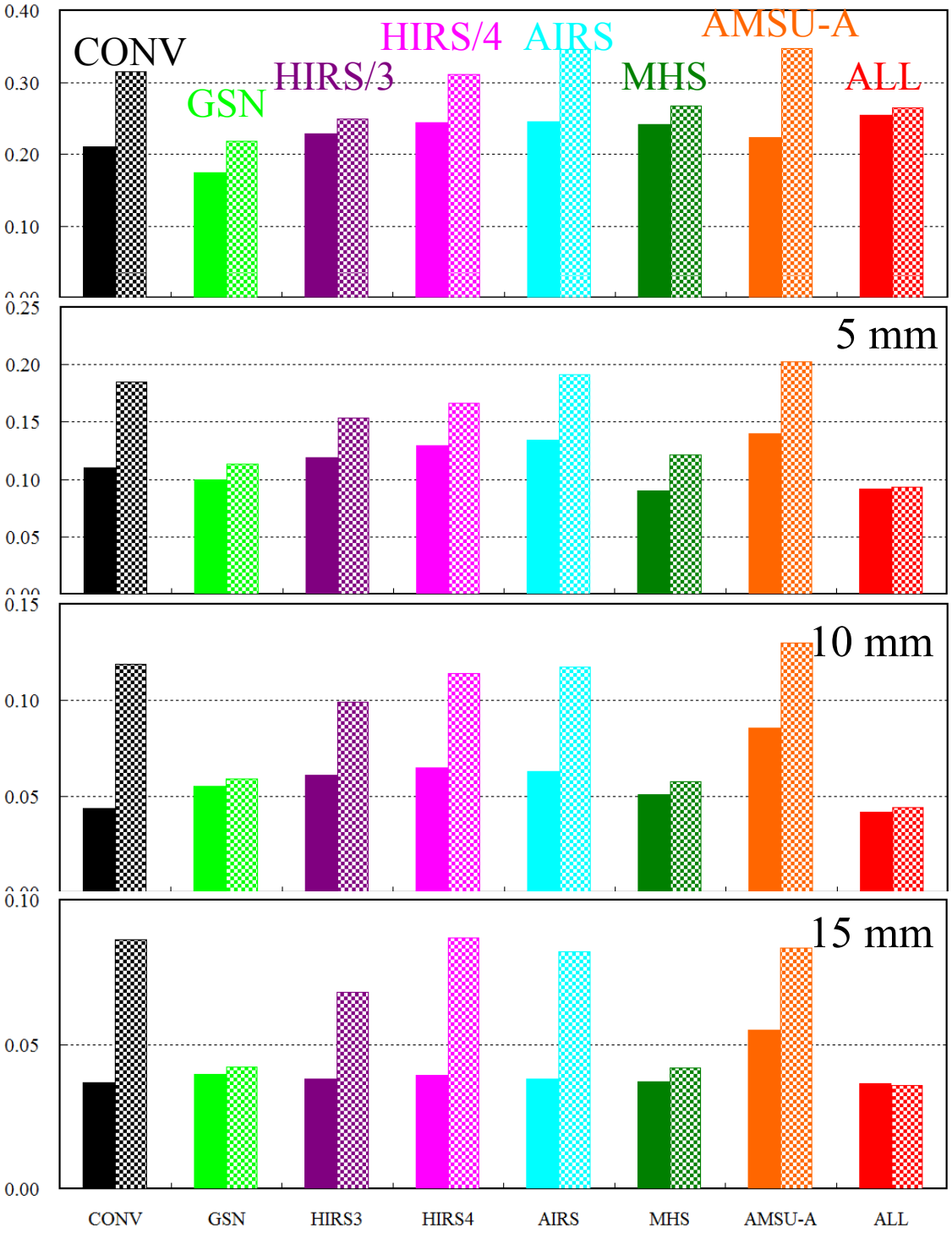

Threat Scores of 3-h Accumulative Rainfall Averaged over 24 Hours

GOES Imager improves the assimilation of a single type of satellite data.

Left bar: without GOES imager
Right bar: with GOES Imager

Verification with GOES Sounder

$$\Delta\sigma = \sigma_{CONV+AMSU-A+GOES\_Img} - \sigma_{CONV+AMSU-A}$$

SNDRD1

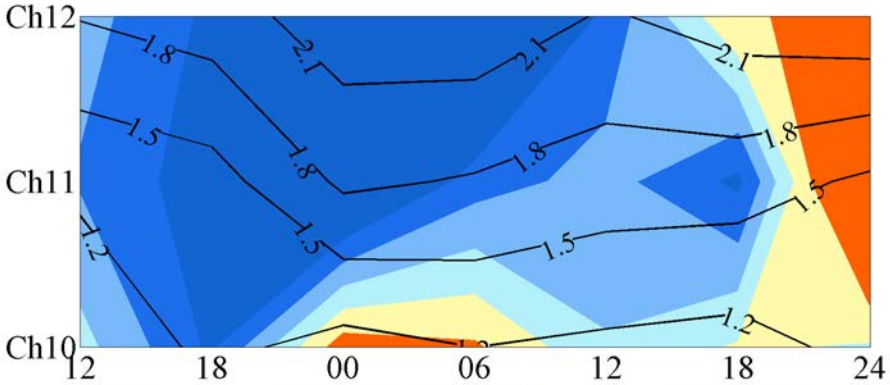

SNDRD2

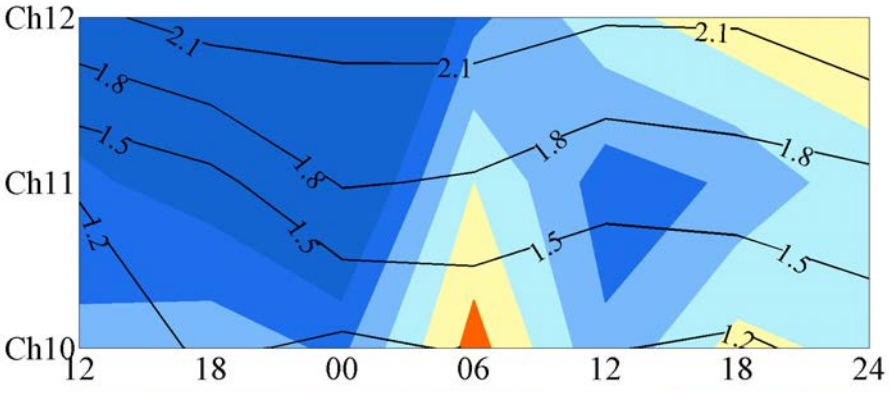

SNDRD3

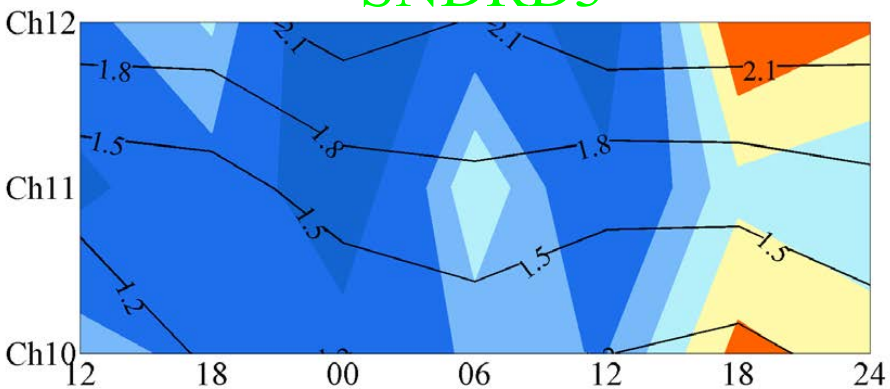

SNDRD4

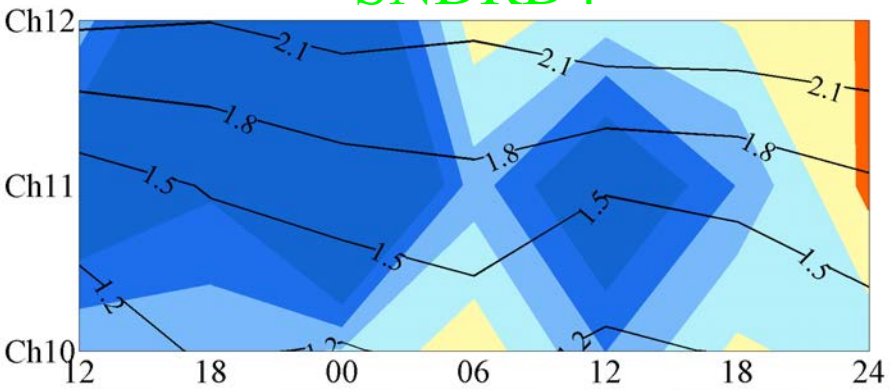

$\Delta\sigma < 0 \leftrightarrow$ Improvement

Verification with Independent GOES Sounder Data

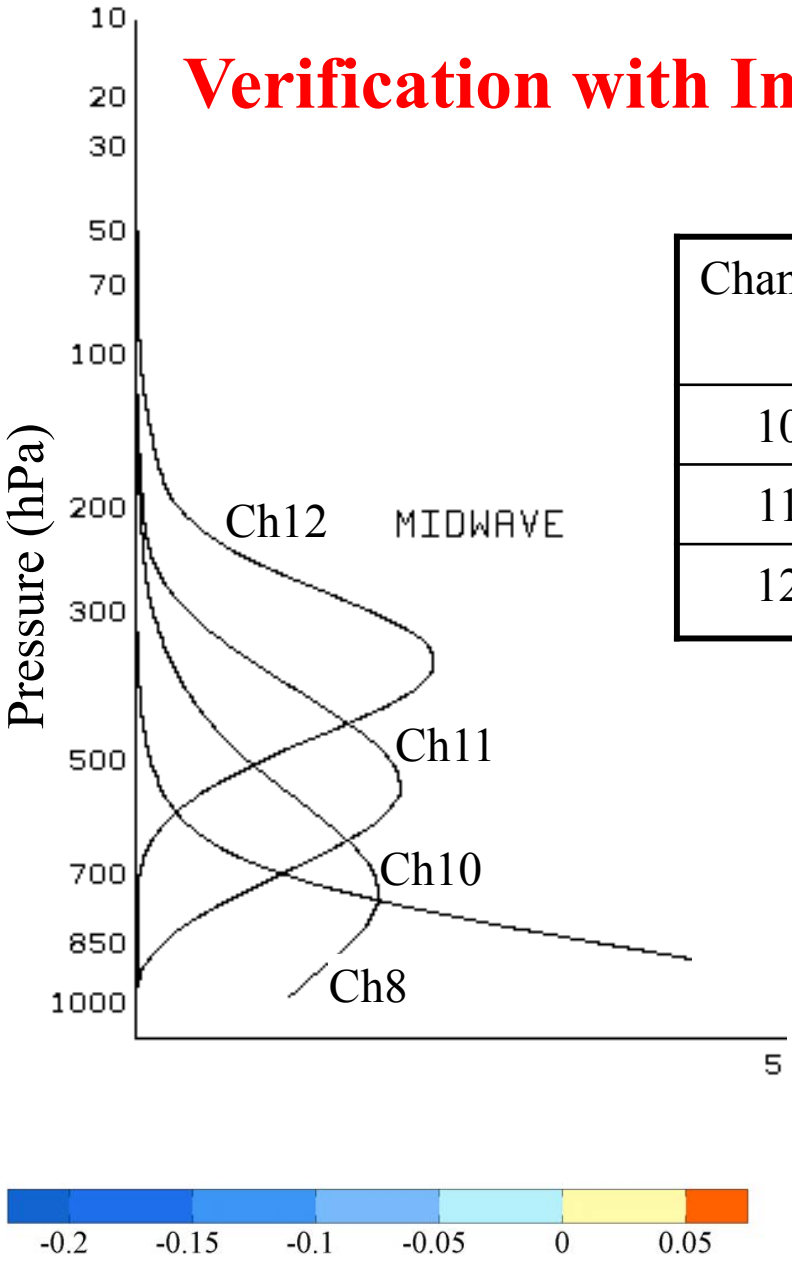

Channel	Wavelength,um (wavenumber, cm^{-1})	Purpose
10	7.43(1345)	Low-level moisture
11	7.02(1425)	Midlevel moisture
12	6.51(1535)	Upper-level moisture

$$\Delta\sigma = \sigma_{CONV+AMSU-A+GOES\_Img} - \sigma_{CONV+AMSU-A}$$

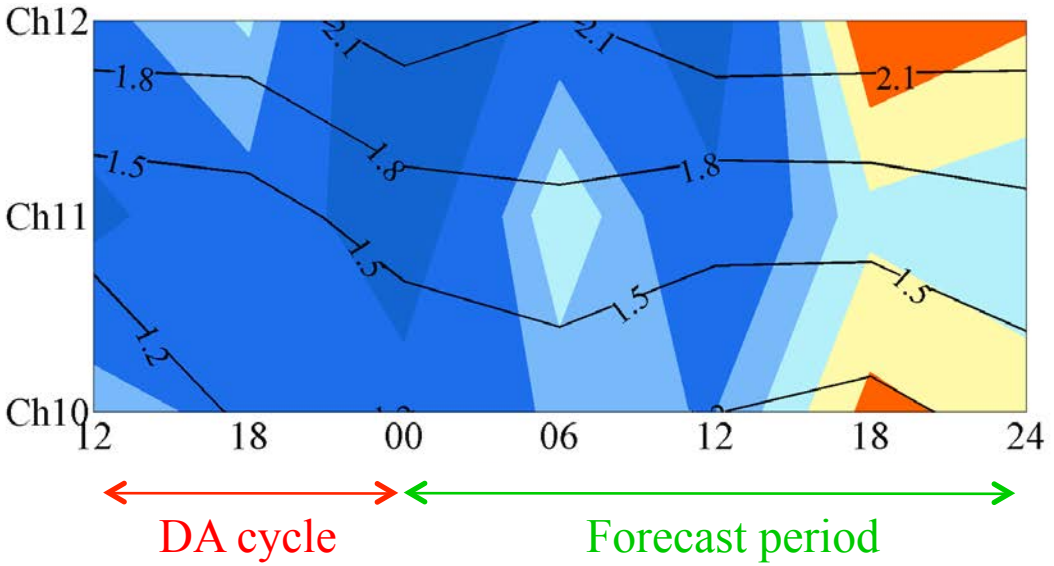

12-h Forecast Verification with AIRS

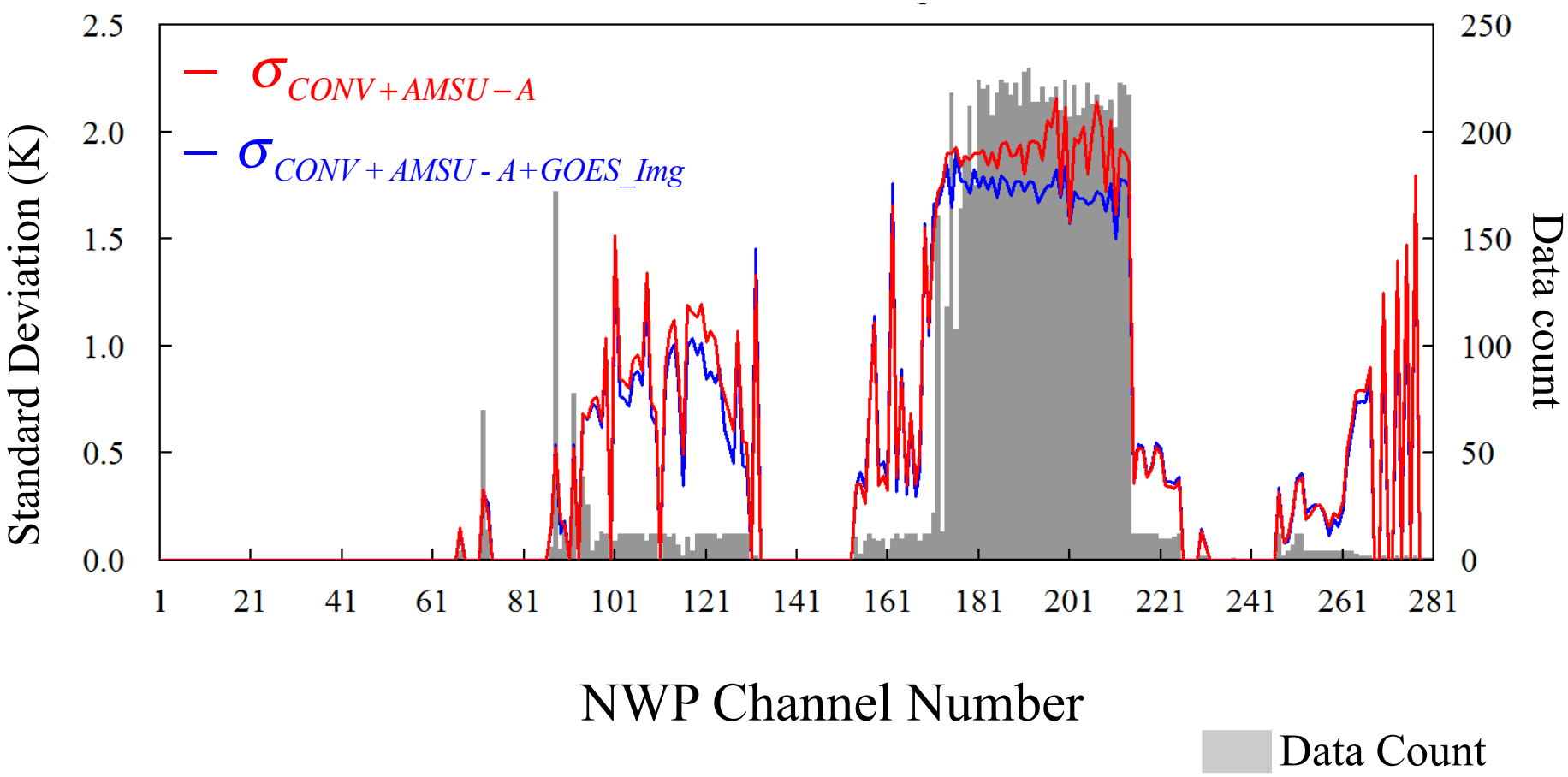

Threat Scores of 3-h Accumulative Rainfall

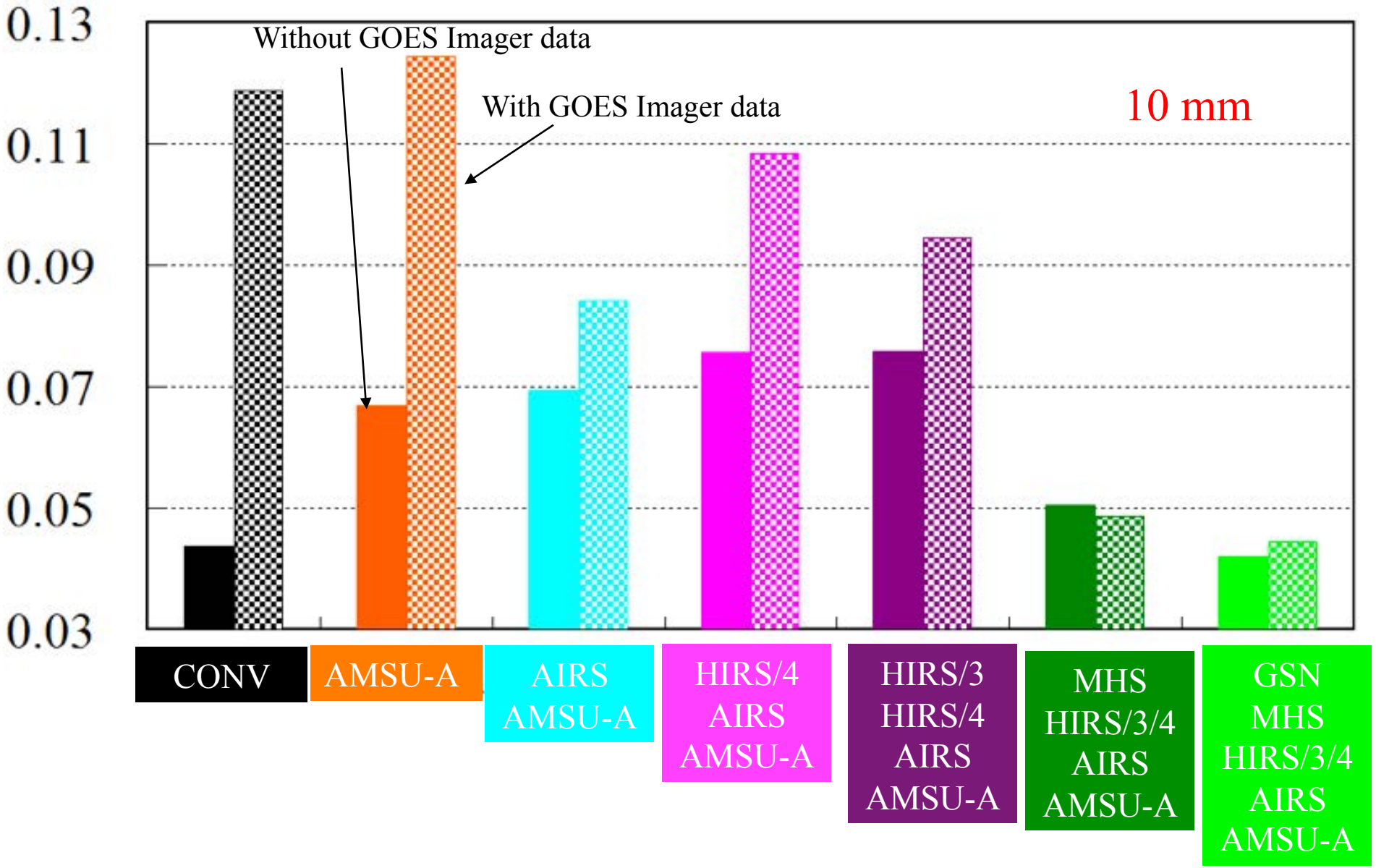

Threat Scores of 3-h Accumulative Rainfall

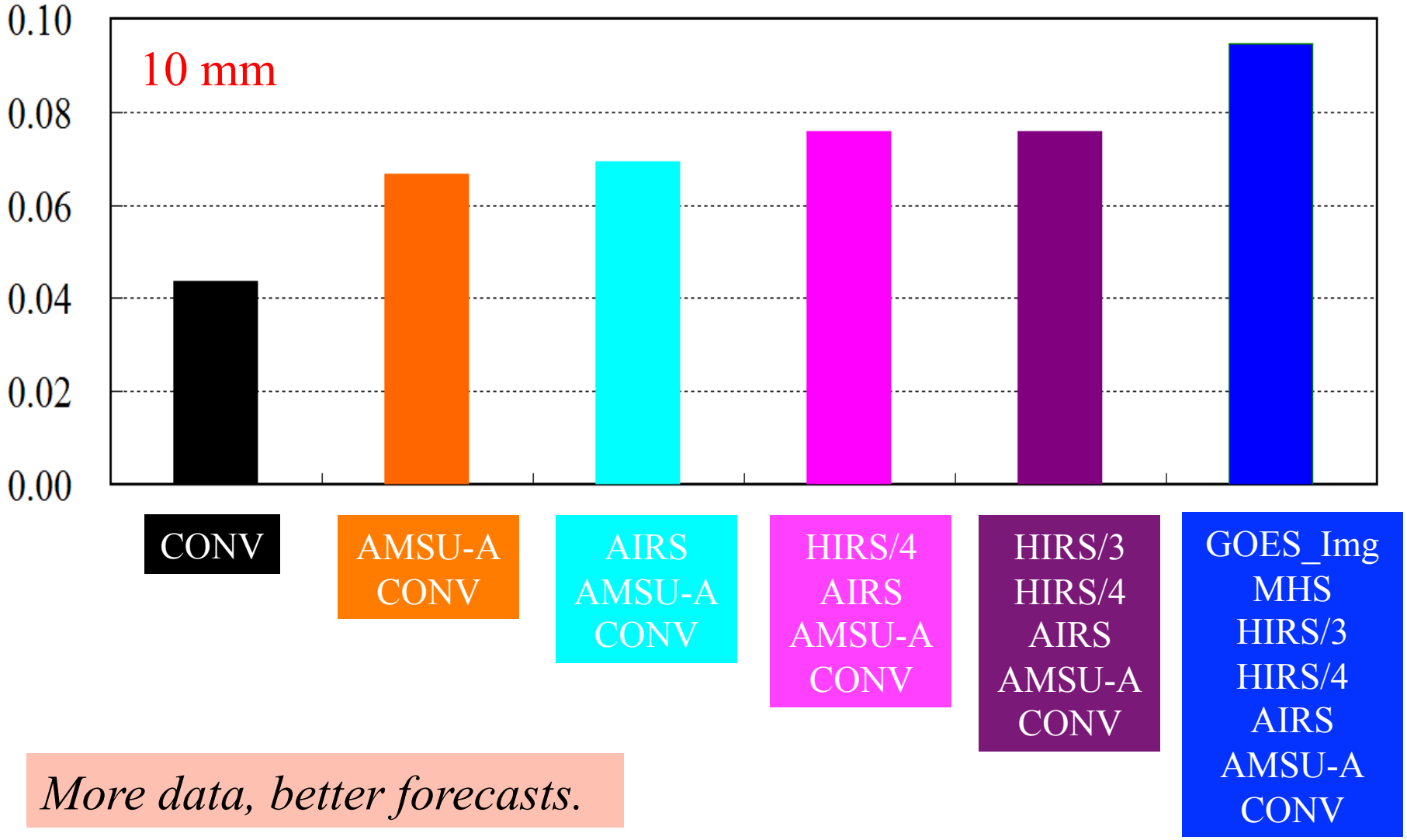

More data, better forecasts.

Threat Scores of 3-h Accumulative Rainfall

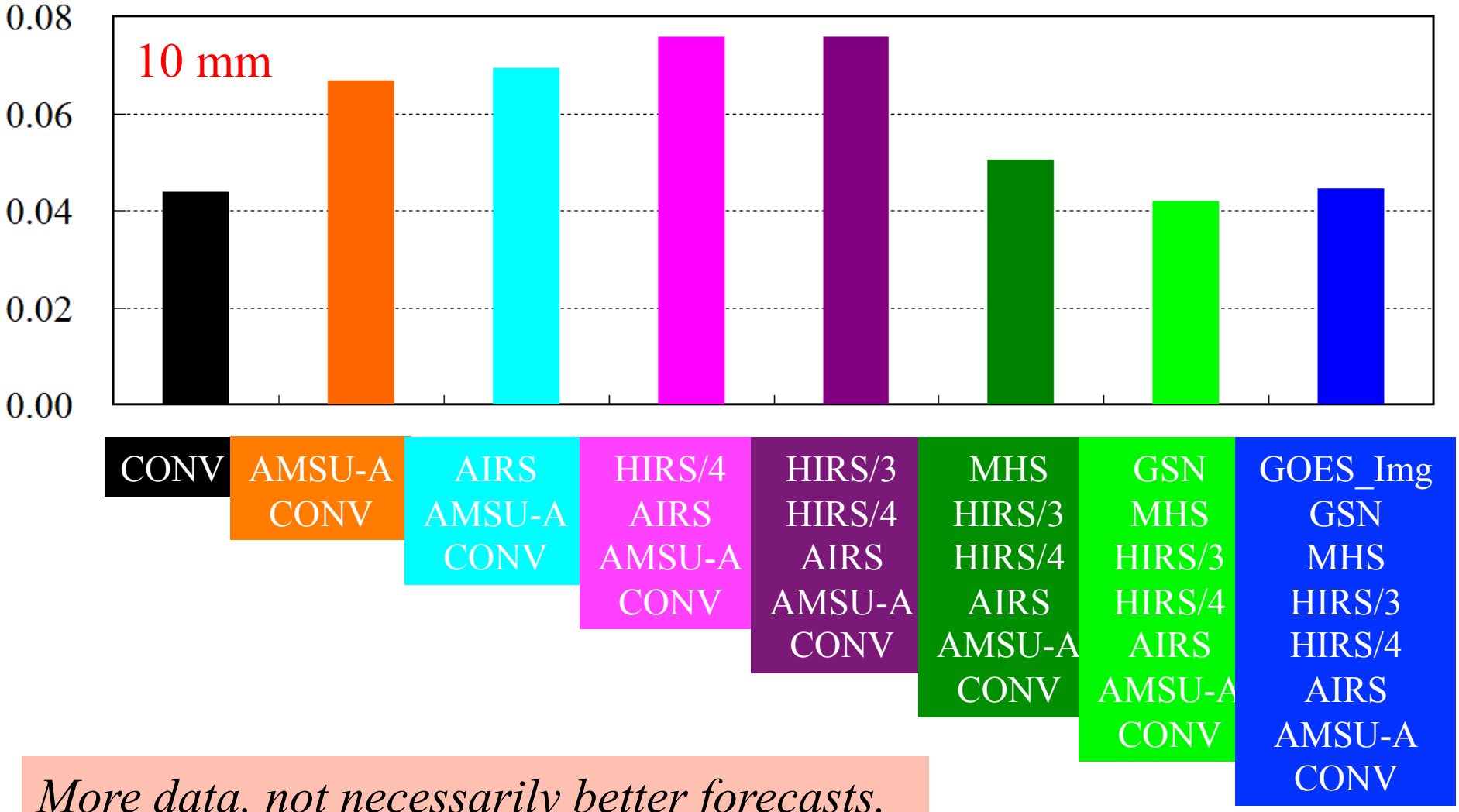

More data, not necessarily better forecasts.

O-B (MHS Channel 3 at 1800 UTC 05/22/08)

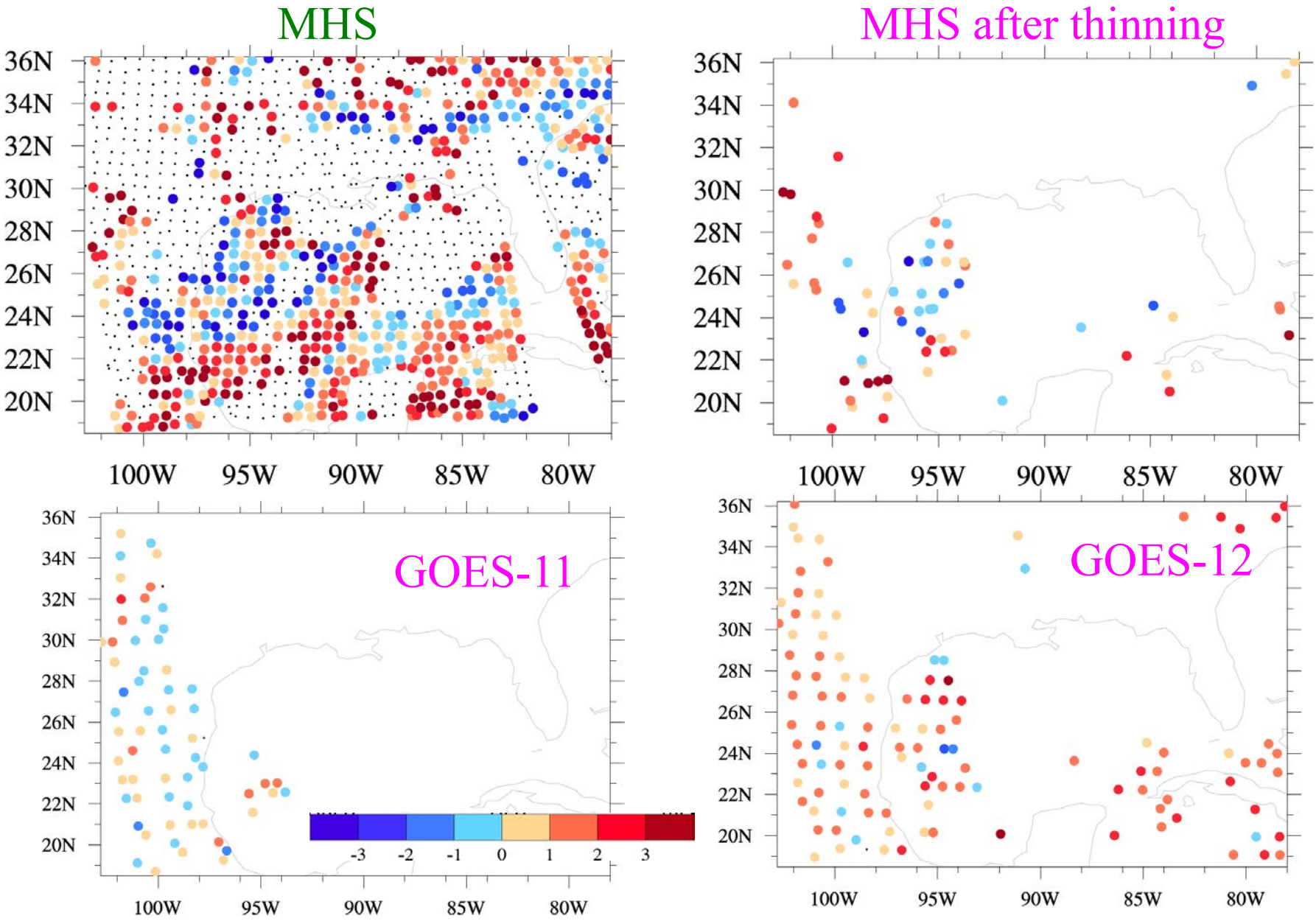

Threat Scores (May 23, 2008)

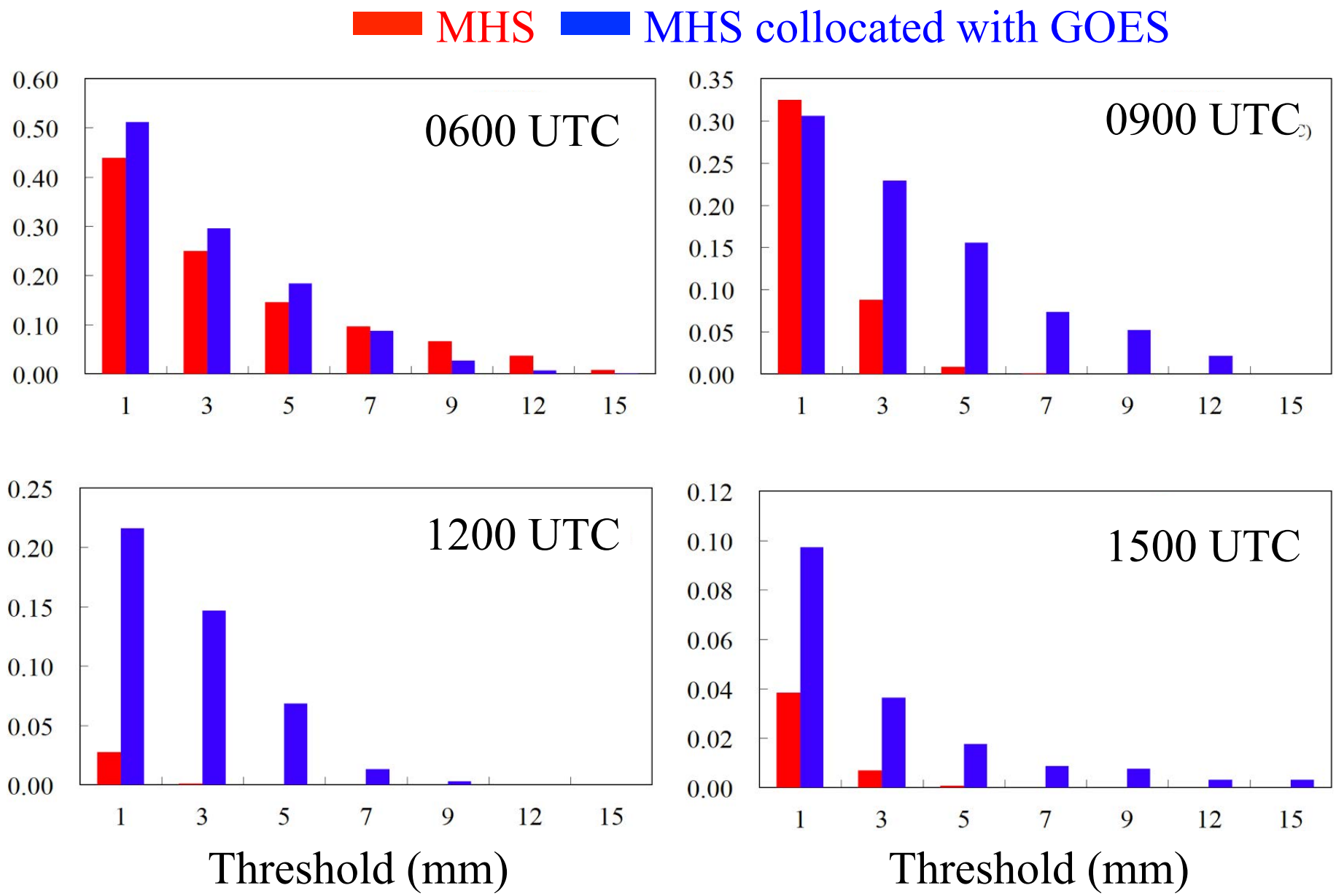

Part II

Improved QPFs by MHS Radiance Data Assimilation with a Newly Added Cloud Detection Algorithm

MHS Data Quality Control (QC)

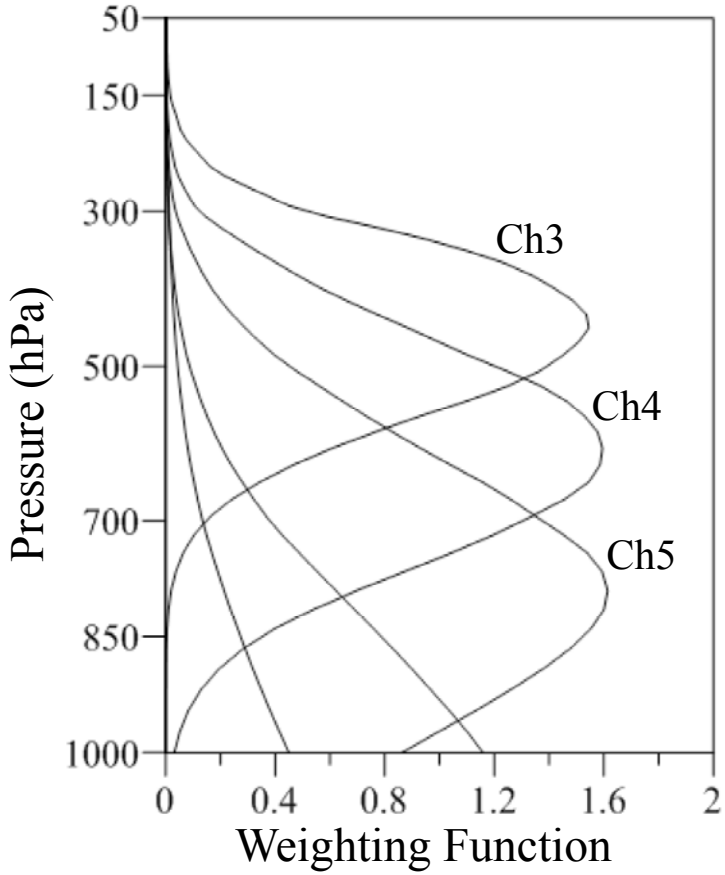

- ✓ MHS QC in GSI and GSI QC results
- ✓ A new MHS QC for cloud detection
- ✓ Impact of the modification of MHS QC to QPFs

LWP Index Used for MHS QC in GSI

Over Ocean:

$$LWP_{index}^{ocean} = \begin{cases} 0.13 \times \left\{ \left(T_{b,1}^{o} - T_{b,1}^{m} \right) - 33.58 \times \dfrac{\left(T_{b,2}^{o} - T_{b,2}^{m} \right)}{300 - T_{b,2}^{o}} \right\}, & \text{if } T_{b,2}^{o} \le 300 \\ 9, & \text{otherwise} \end{cases}$$

Over Land:

$$LWP_{index}^{land} = 0.85 \times \left(T_{b,1}^{o} - T_{b,1}^{m} \right) - \left(T_{b,2}^{o} - T_{b,2}^{m} \right)$$

$$\left.\begin{array}{l} T_{b,1}^{o} - T_{b,1}^{m} \\ T_{b,2}^{o} - T_{b,2}^{m} \end{array}\right\}$$ O-B differences of MHS channels 1-2

$TPW_{index} > 1$ Three Steps for MHS Data Rejection in GSI

Step I:

$$TPW_{index} \equiv \left\{ \left[\left(T_{b,1}^{o} - T_{b,1}^{m} \right) - 7.5 \times LWP_{index} \right] / 10.0 \right\}^2 + LWP_{index}^2 > 1$$

Step II:

$$\left| O - B \right| > 3 \left(e_i \times \left(1 - TPW_{index}^2 \right) \times f_H \times \tau_i^{top} \right)$$

or: $\left| O - B \right| > 6\text{K}$

e_i is accuracy of obs.

f_H=2000/H, H is terrain height>2km

τ_i^{top} is ransmittance at model top

Step III:

All five channels if data of any other channel was removed by the first two QC steps

Diagnosis of MHS QC Results

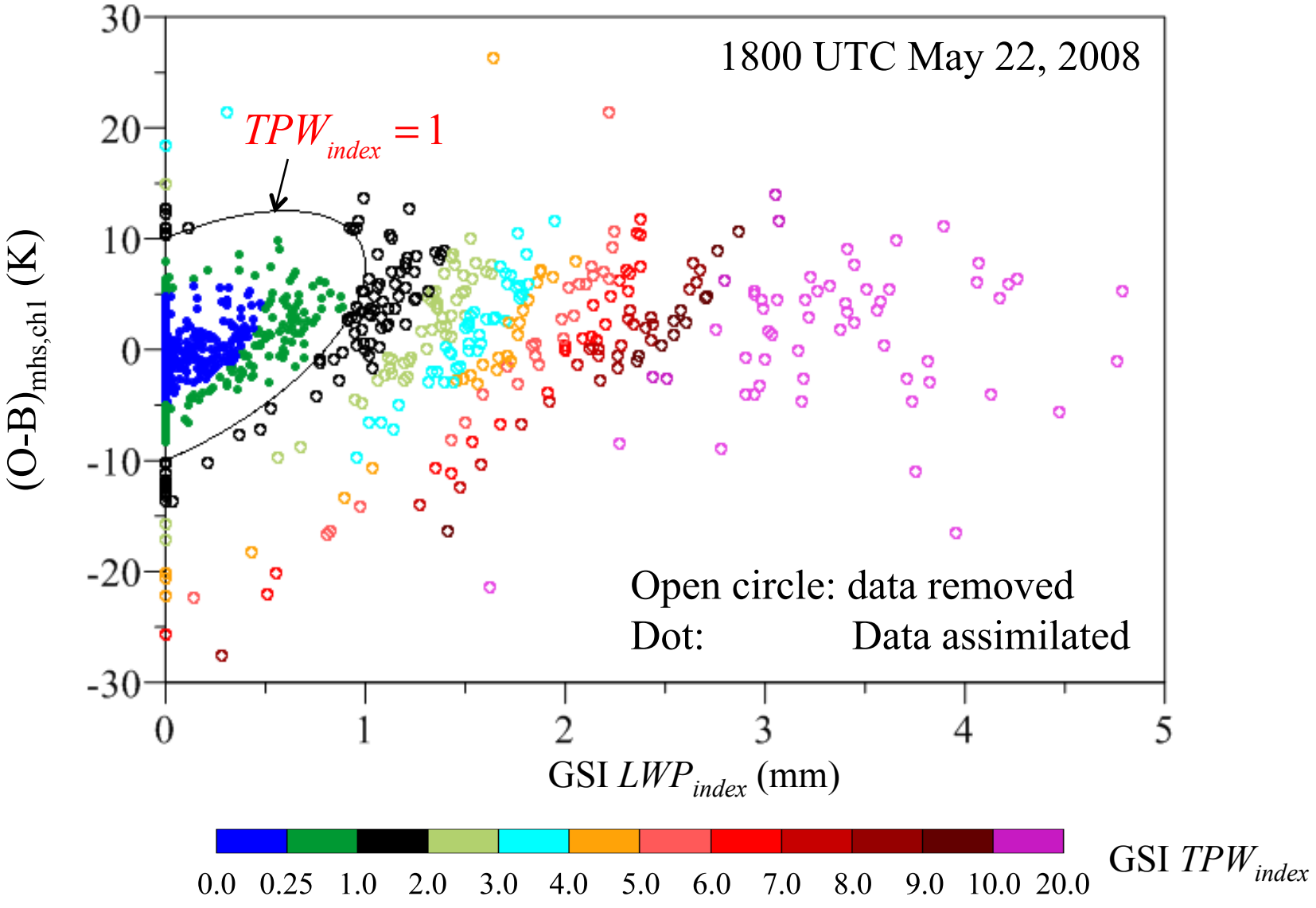

Diagnosis of MHS QC Results (cont.)

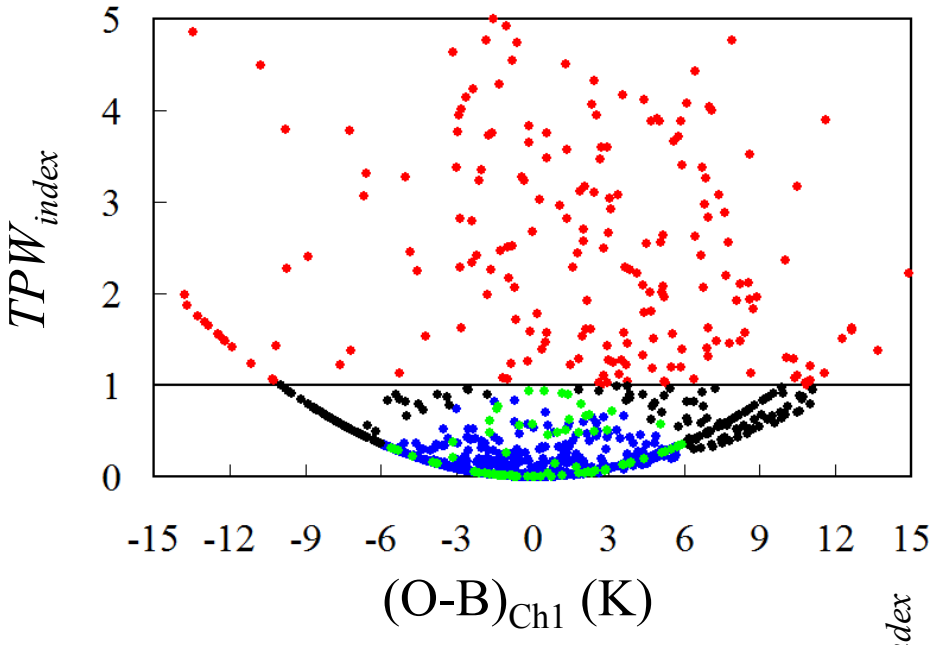

Data eliminated by

- Step I defined by TPW_{index}
- Step II defined by O-B
- Step III defined by inter-channels relationship

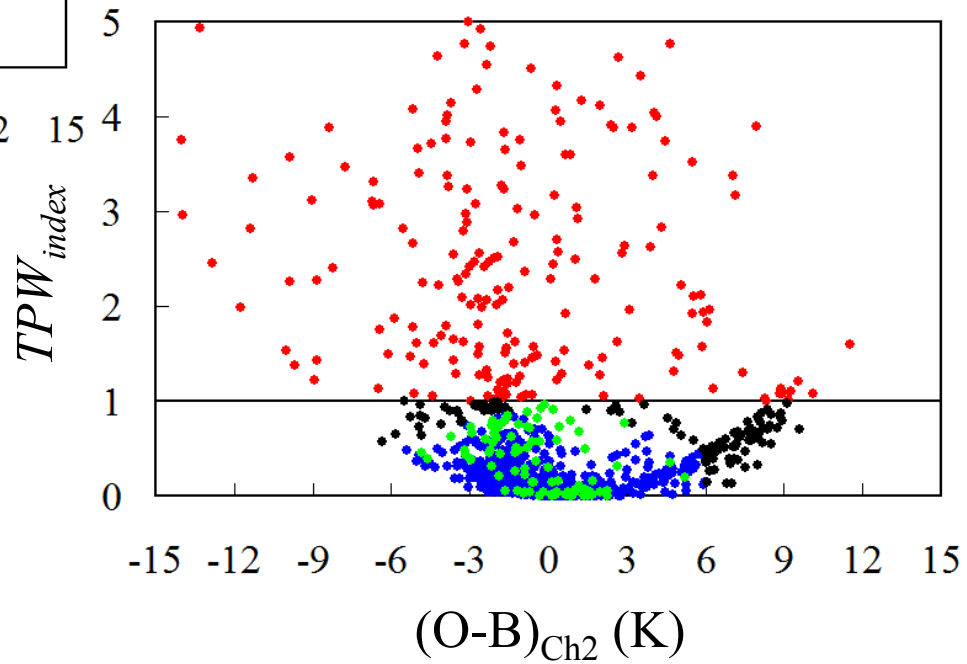

1800 UTC May 22, 2008

Diagnosis of MHS GSI QC

Data that pass GSI QC

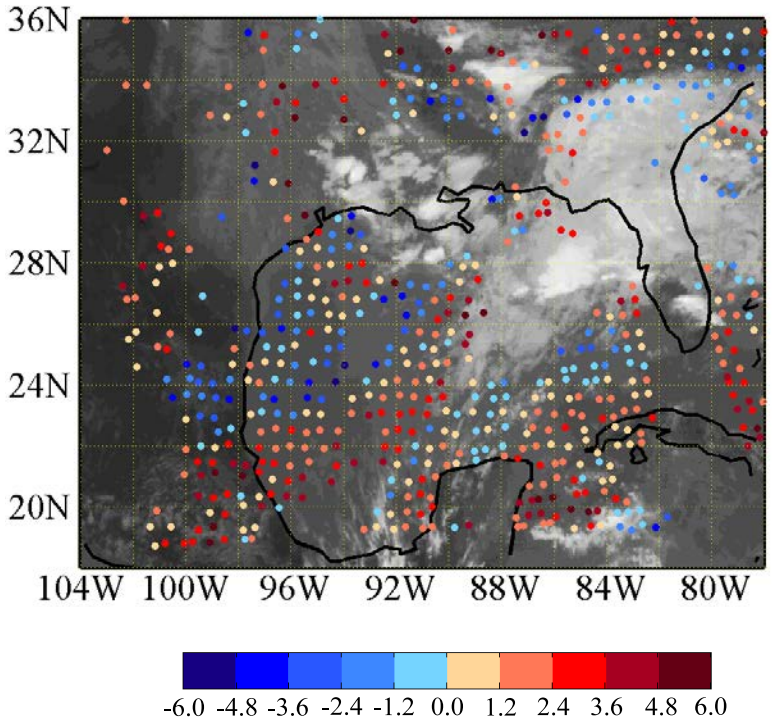

MHS O-B

Modeled RH at 300 hPa

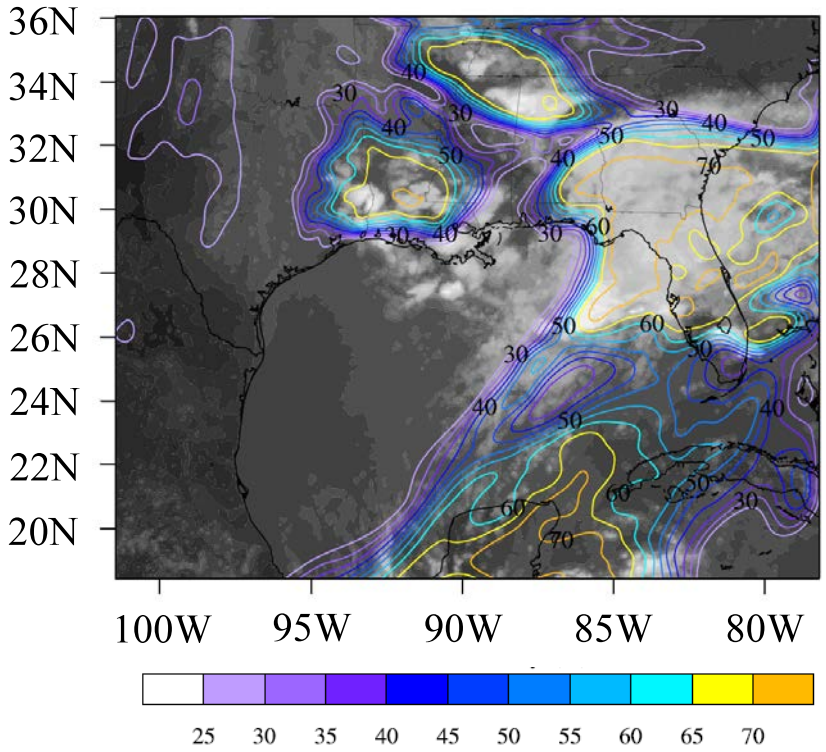

RH at 300-hPa

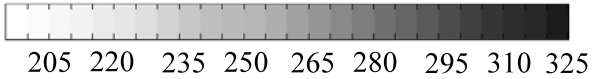

GOES 10.7μm

Infrared O-B More Sensitive to Cloud Than Microwave

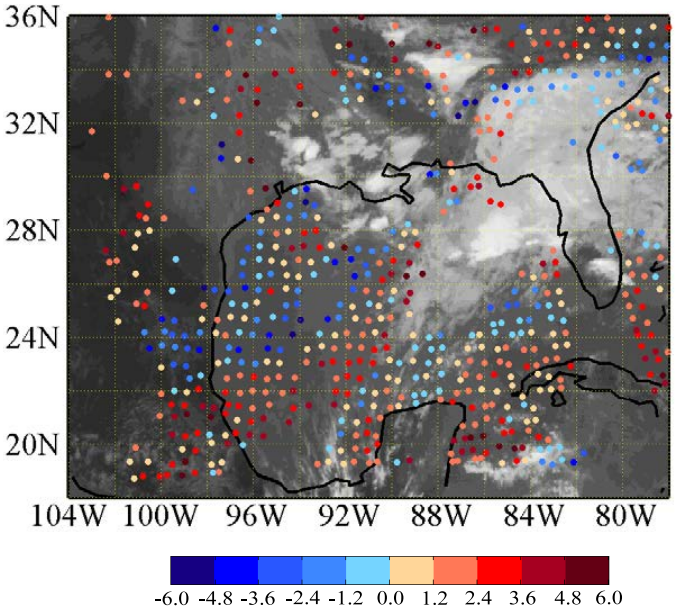

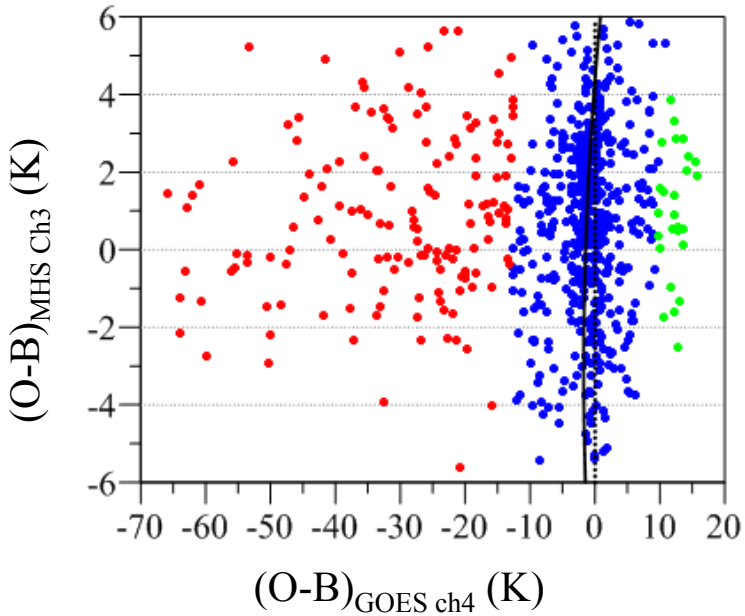

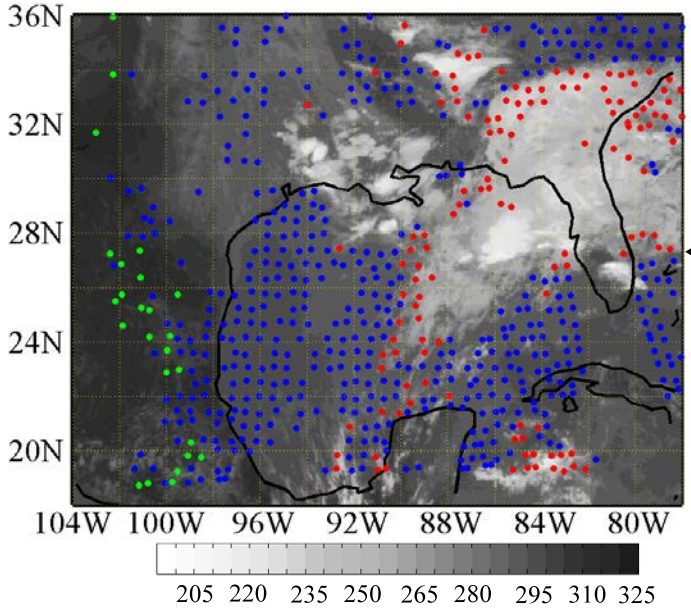

"$(O\text{-}B)_{GOES}$" Regressed by MHS Channels 1, 2 and 5

Over Ocean:

$$(O-B)^{regression}_{GOES,ch4} = -0.536 \times T^{obs}_{b,MHS_{ch1}} + 1.132 \times T^{obs}_{b,MHS_{ch2}} + 0.537 \times T^{obs}_{b,MHS_{ch5}} - 321.318$$

Over Land:

$$(O-B)^{regression}_{GOES,ch4} = 0.009 \times T^{obs}_{b,MHS_{ch1}} + 0.085 \times T^{obs}_{b,MHS_{ch2}} + 0.877 \times T^{obs}_{b,MHS_{ch5}} - 274.255$$

Observations of MHS channels 1-2, 5 are used in the regression.

- Channels 1-2 are affected by the radiation from both the Earth's surface and emission and scattering from ice phase clouds
- Channel 5 is most sensitive to scattering from thin clouds

Thresholds for Cloud Detection

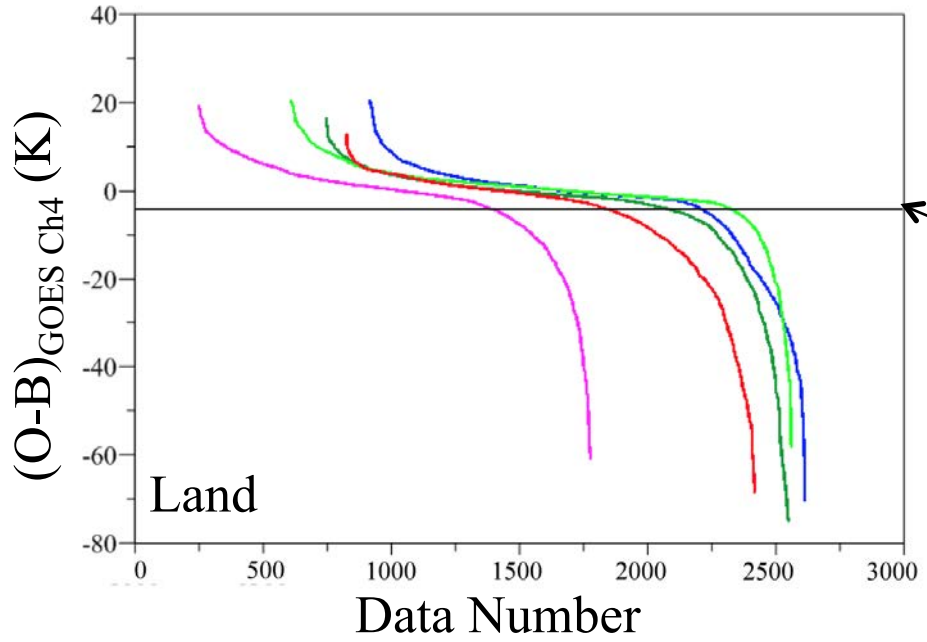

$$(O-B)^{regression}_{GOES,land} \le -4K$$

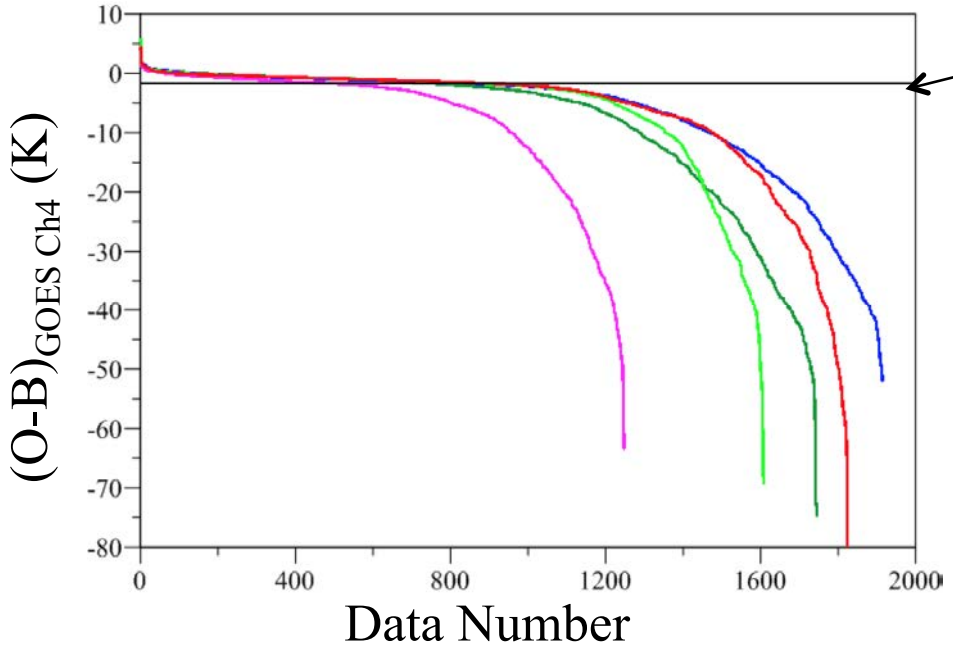

$$(O-B)^{regression}_{GOES,ocean} \le -2K$$

MHS data from NOAA-18 on May 17, 18, 19, 20, 21, 2008

O-B Scatter Plots for MHS Channels 1-5 versus GOES-12 Ch4

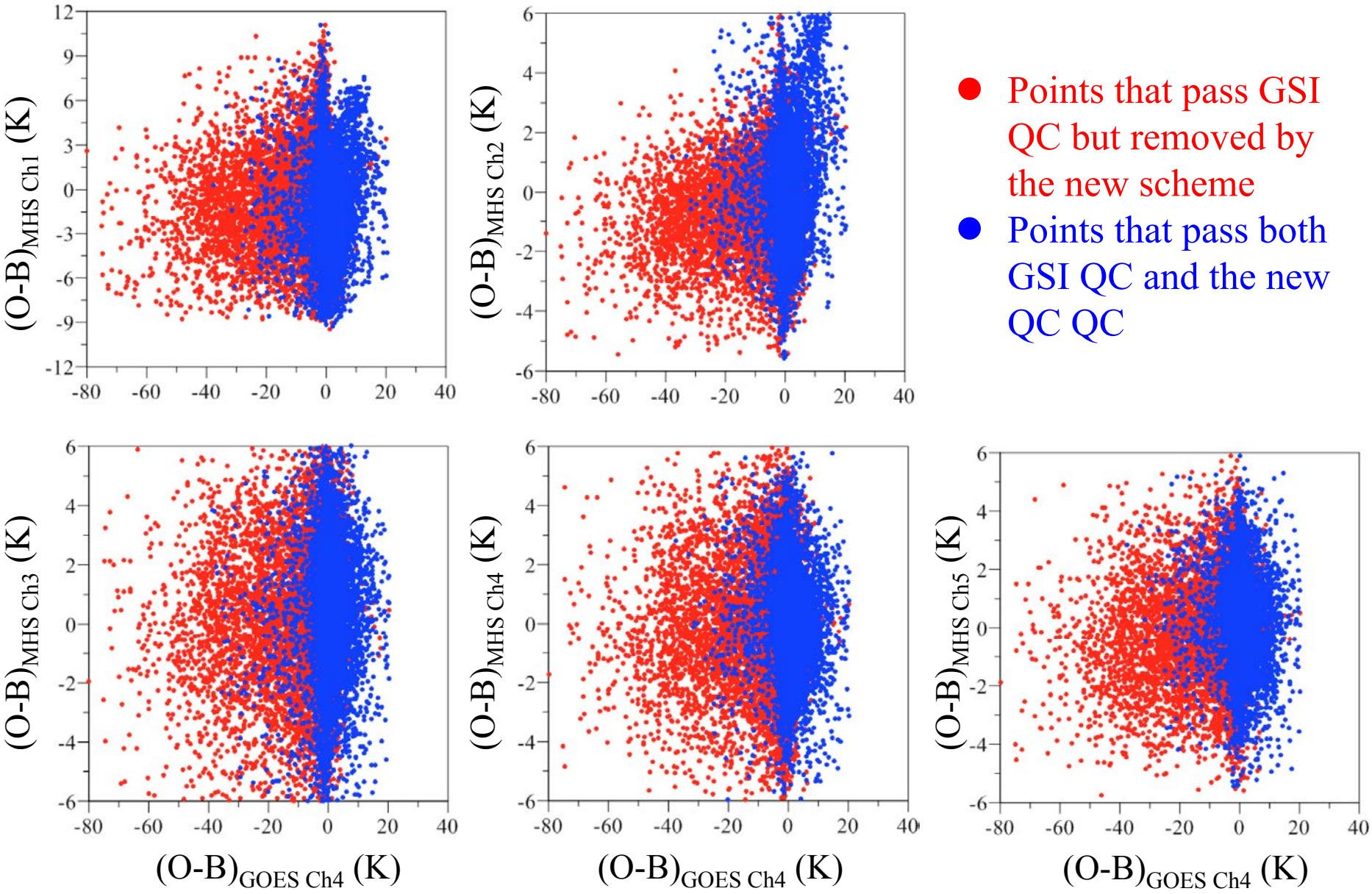

- Points that pass GSI QC but removed by the new scheme
- Points that pass both GSI QC and the new QC QC

24-h QPFs of 3-h Accumulative Rainfall

EXP1: The original GSI QC for MHS data is used.

May 23, 2008

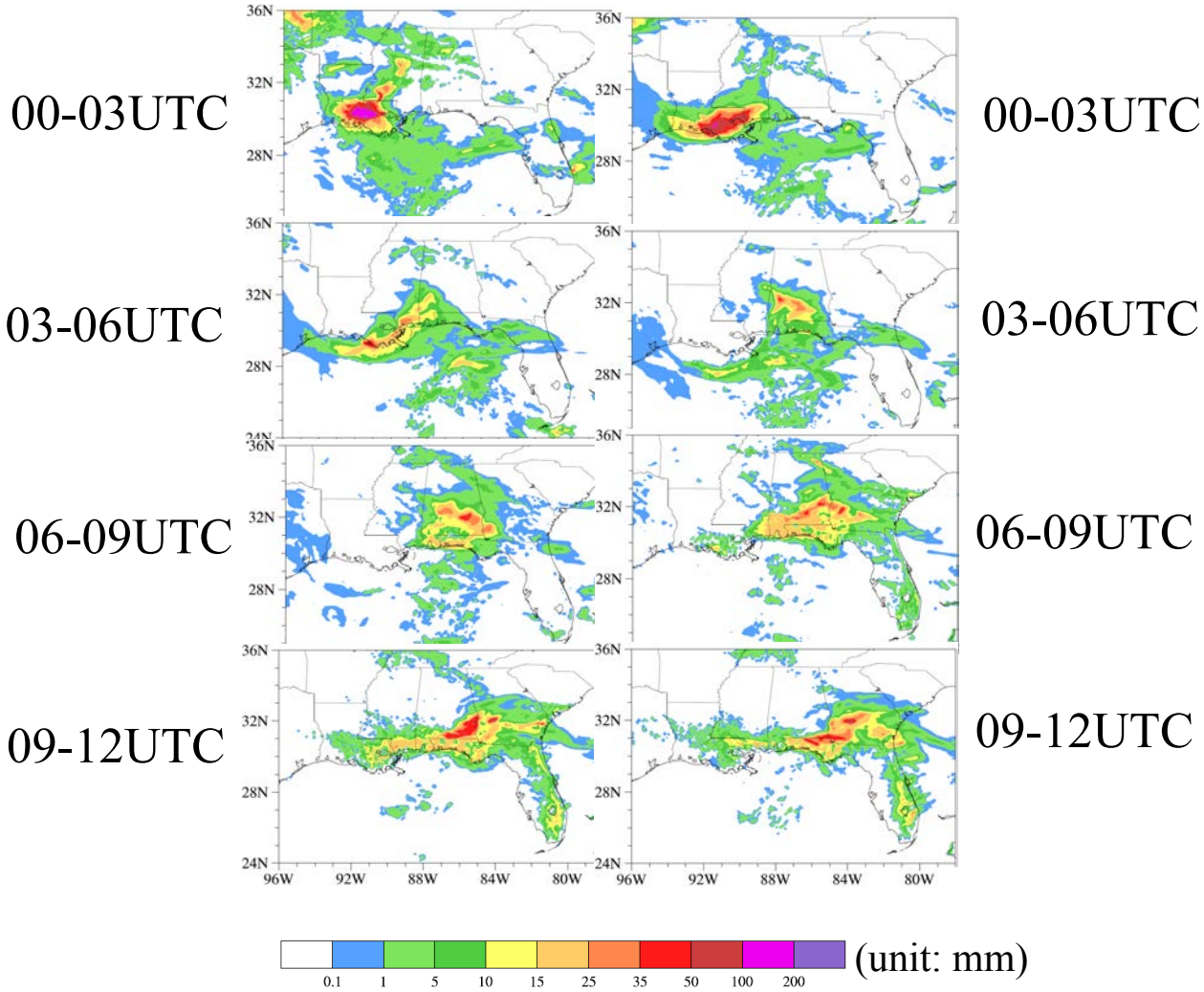

24-h Forecasts of 3-h Accumulative Rainfall

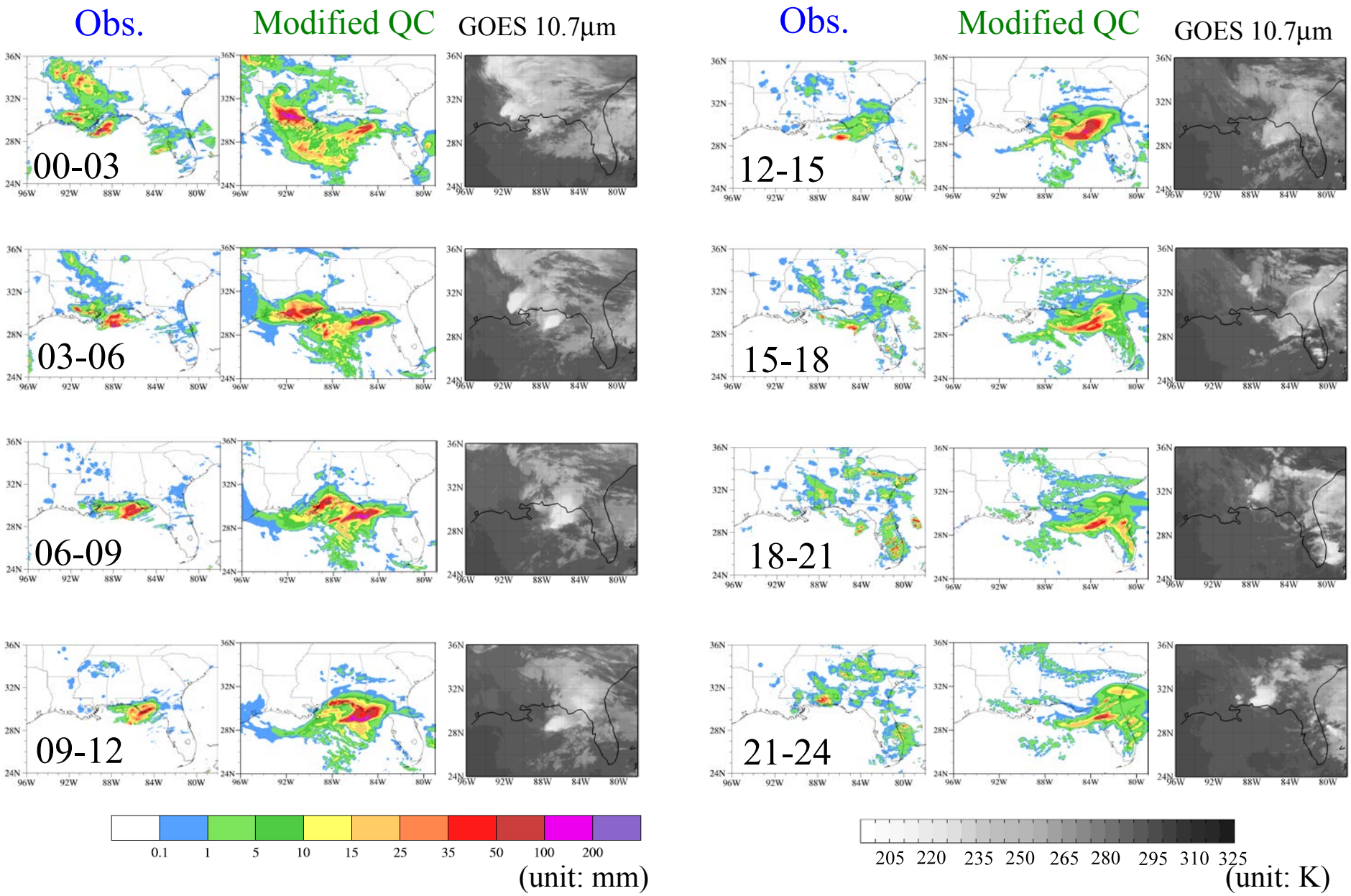

Threat scores (TS) of 3-hour Accumulative Rainfall

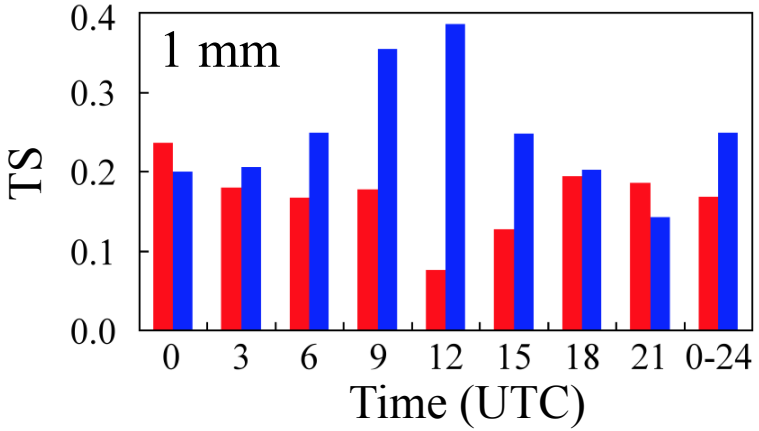

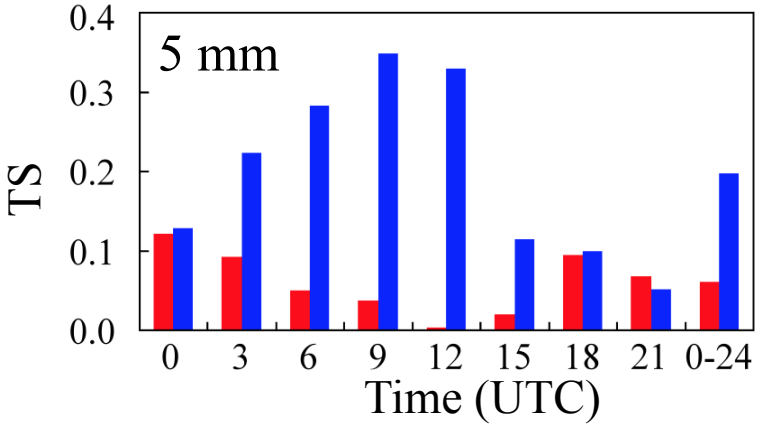

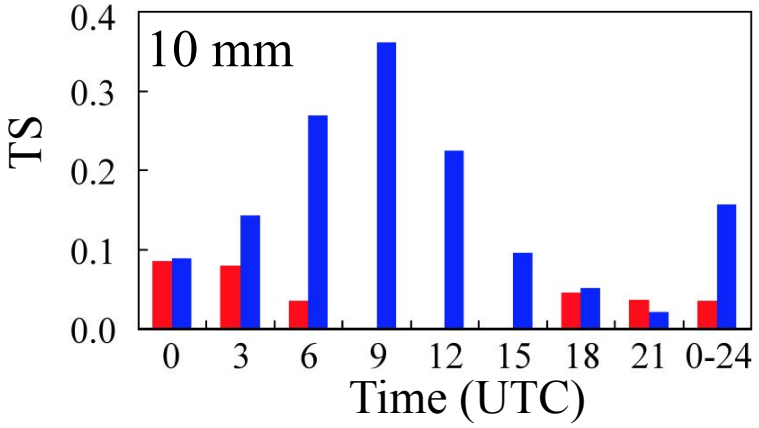

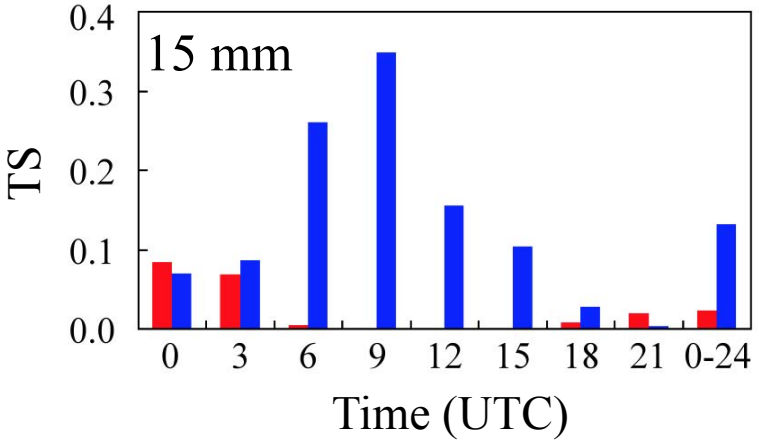

EXP1:CONV+AMSU-A+MHS

EXP2:Same as EXP1 except for modified MHS QC

Part III

Impacts of ATMS Data Assimilation on Hurricane Track and Intensity Forecasts

Suomi NPP Satellite Instruments

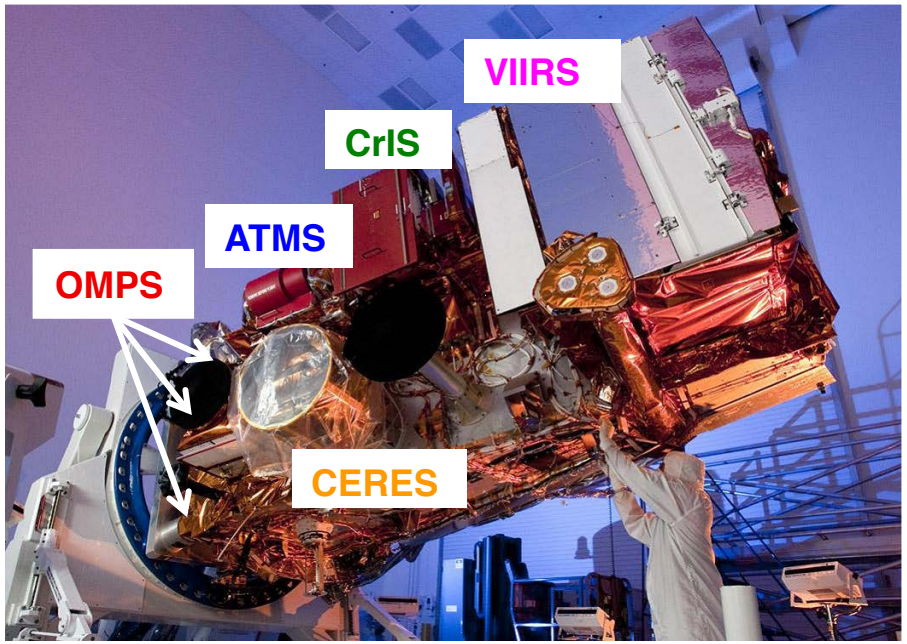

ATMS --- Advanced Technology Microwave Sounder

CrIS --- Cross-track Infrared Sounder

VIIRS --- Visible/Infrared Imager/Radiometer Suite

OMPS --- Ozone Mapping and Profiler Suite

CERES --- Cloud and Earth Radiant Energy System

Channel Characteristics of ATMS and AMSU

Channel		Frequency (GHz)		NEΔT (K)		Beam width (°)		Peak WF (hPa)	
ATMS	AMSU	ATMS	AMSU	ATMS	AMSU	ATMS	AMSU	ATMS	AMSU
1		23.8		0.50	0.30	5.2	3.3	Surface	
2		31.4	31.399	0.60	0.30	5.2	3.3	Surface	
3		50.3	50.299	0.70	0.40	2.2	3.3	Surface	
4		51.76		0.50		2.2		Surface	
5	4	52.8		0.50	0.25	2.2	3.3	1000	
6	5	53.596±0.115		0.50	0.25	2.2	3.3	700	
7	6	54.4		0.50	0.25	2.2	3.3	400	
8	7	54.94		0.50	0.25	2.2	3.3	270	
9	8	55.5		0.50	0.25	2.2	3.3	180	
10	9	57.29		0.75	0.25	2.2	3.3	90	
11	10	57.29± 0.217		1.00	0.40	2.2	3.3	50	
12	11	57.29± 0.322± 0.048		1.00	0.40	2.2	3.3	25	
13	12	57.29± 0.322 ± 0.022		1.25	0.60	2.2	3.3	12	
14	13	57.29± 0.322 ± 0.010		2.20	0.80	2.2	3.3	5	
15	14	57.29± 0.322± 0.0045		3.60	1.20	2.2	3.3	2	
16	15	88.2	89.0	0.30	0.50	2.2	3.3	Surface	
17	16	165.5	89.0	0.60	0.84	1.1	1.1	1000	Surface
18	17	183.31±7.0	157.0	0.80	0.84	1.1	1.1	800	Surface
19	18	183.31±4.5	183.31±1.0	0.80	0.60	1.1	1.1	700	400
20	19	183.31±3.0		0.80	0.70	1.1	1.1	600	
21	20	183.31±1.8	183.31±7.0	0.80	1.06	1.1	1.1	500	800
22		183.31±1.0		0.90		1.1		400	

ATMS Weighting Functions and HWRF Model Levels

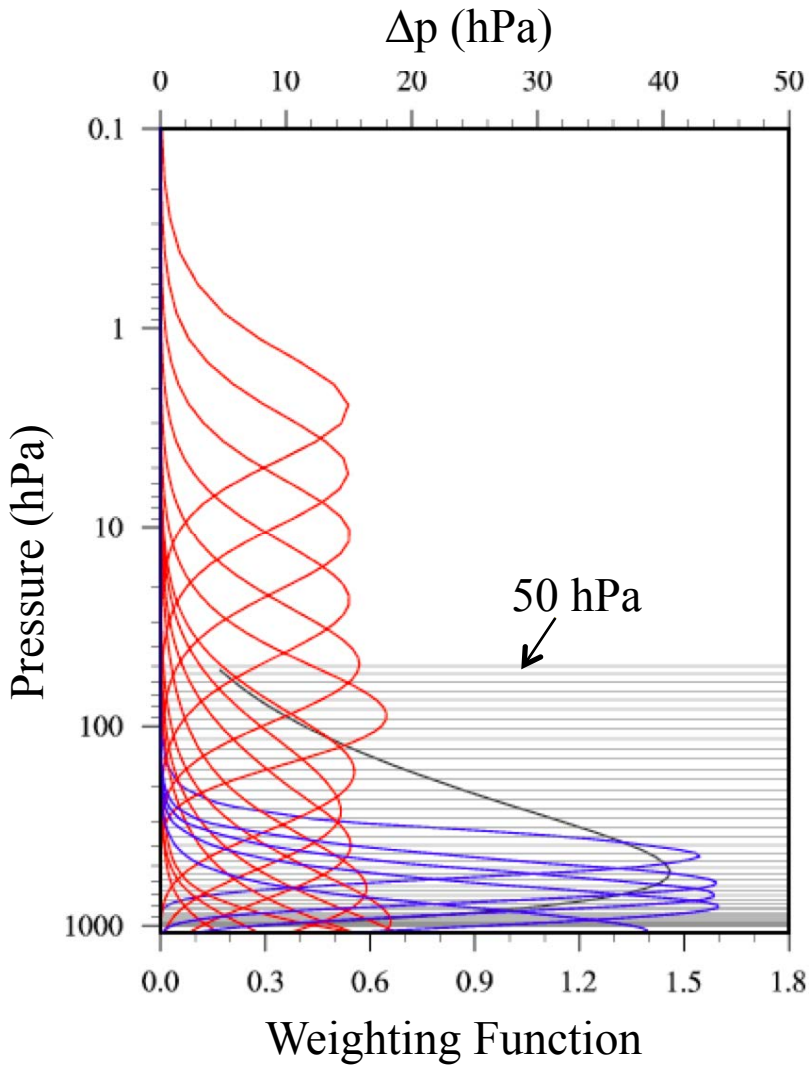

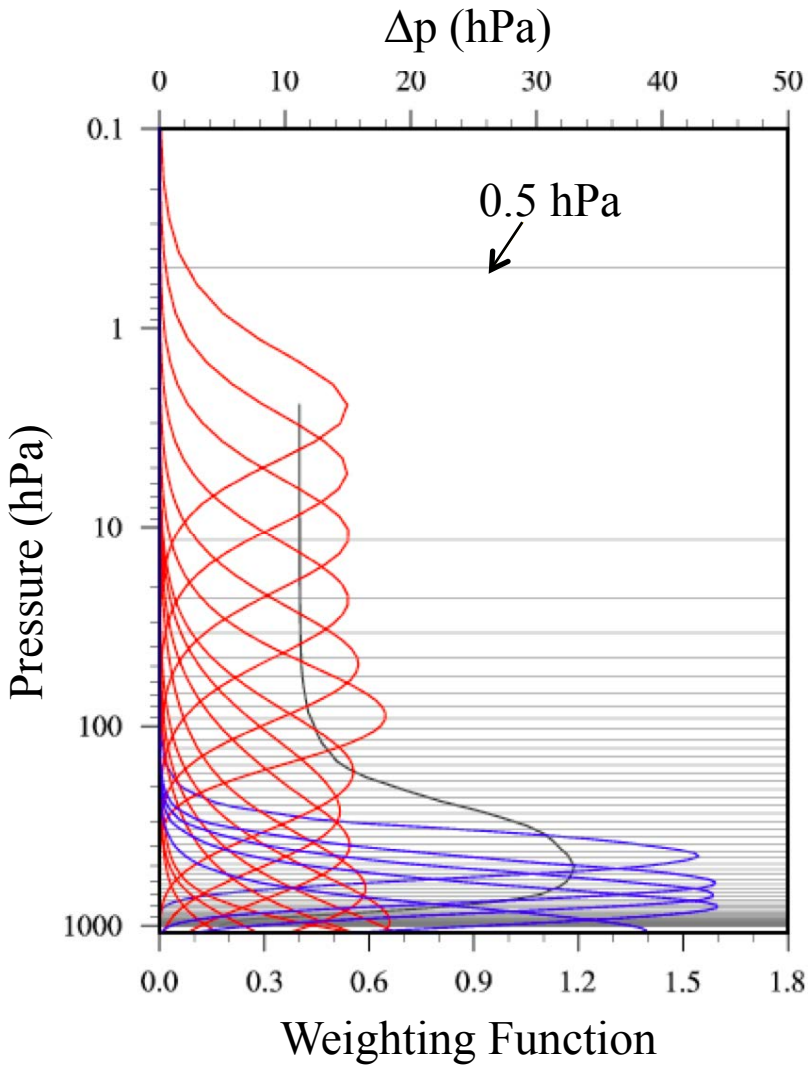

Same FOVs for All ATMS Channels

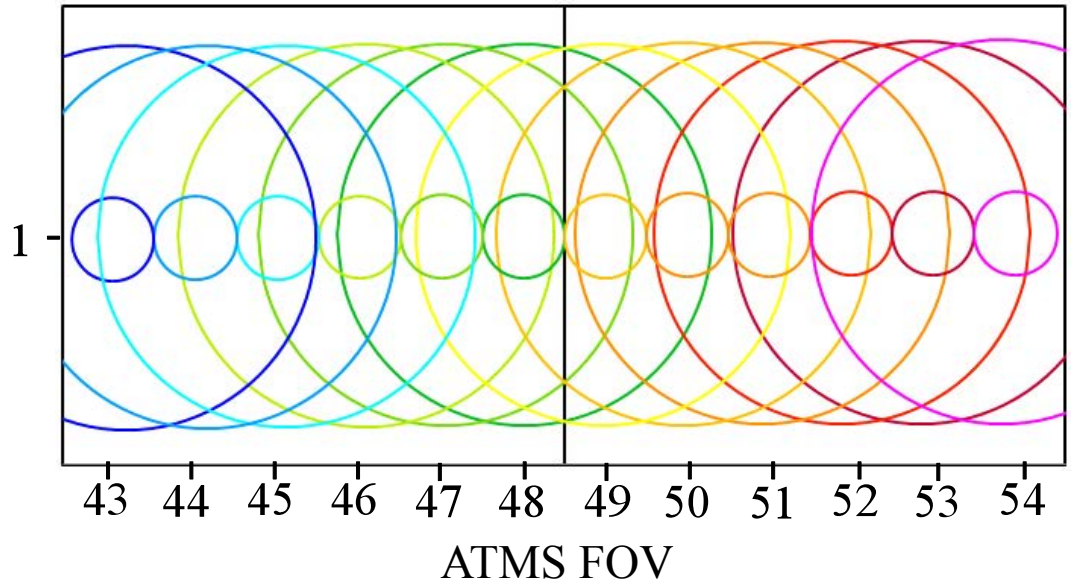

Channels 1-2 (larger FOV)

Channels 17-22 (smaller FOV)

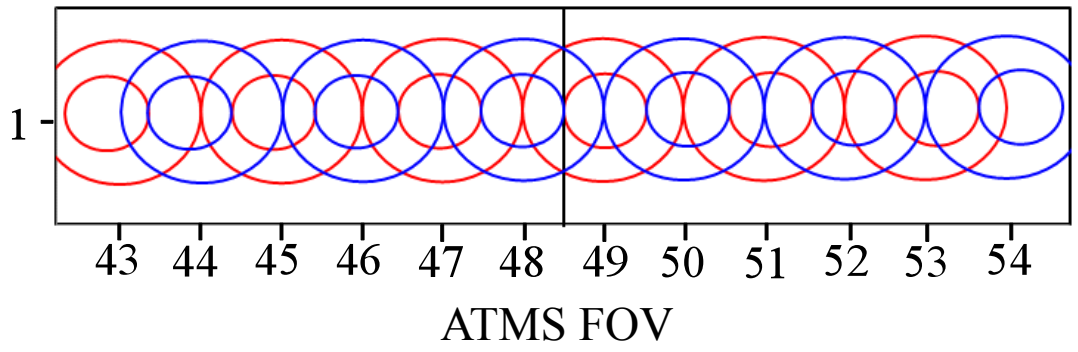

Channels 3-16 (larger FOV)

Channels 17-22 (smaller FOV)

A consistent FOV distribution between temperature and humidity channels on ATMS makes the cloud detection easy to implement.

Inconsistent FOVs between AMSU-A and MHS

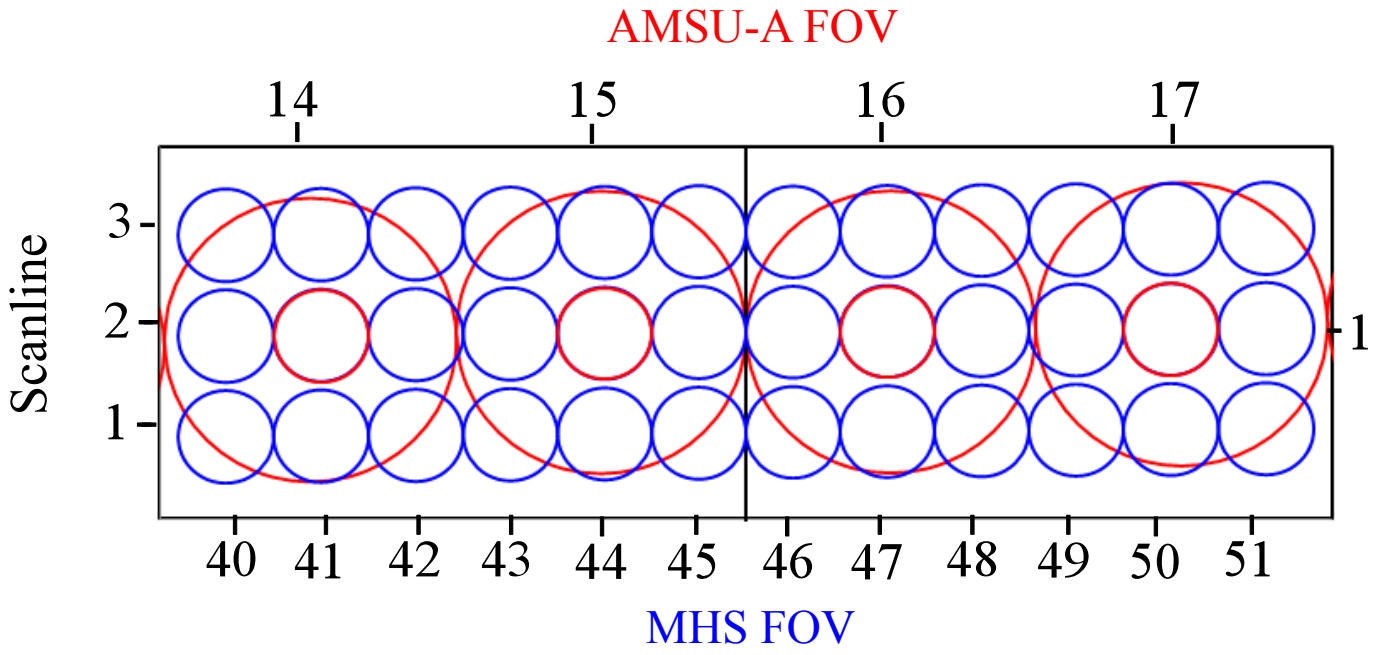

An inconsistent FOV distribution between AMSU-A and MHS channels makes the cloud detection for MHS data difficult.

The outer domain, ghost domain, middle nest and inner nest of HWRF

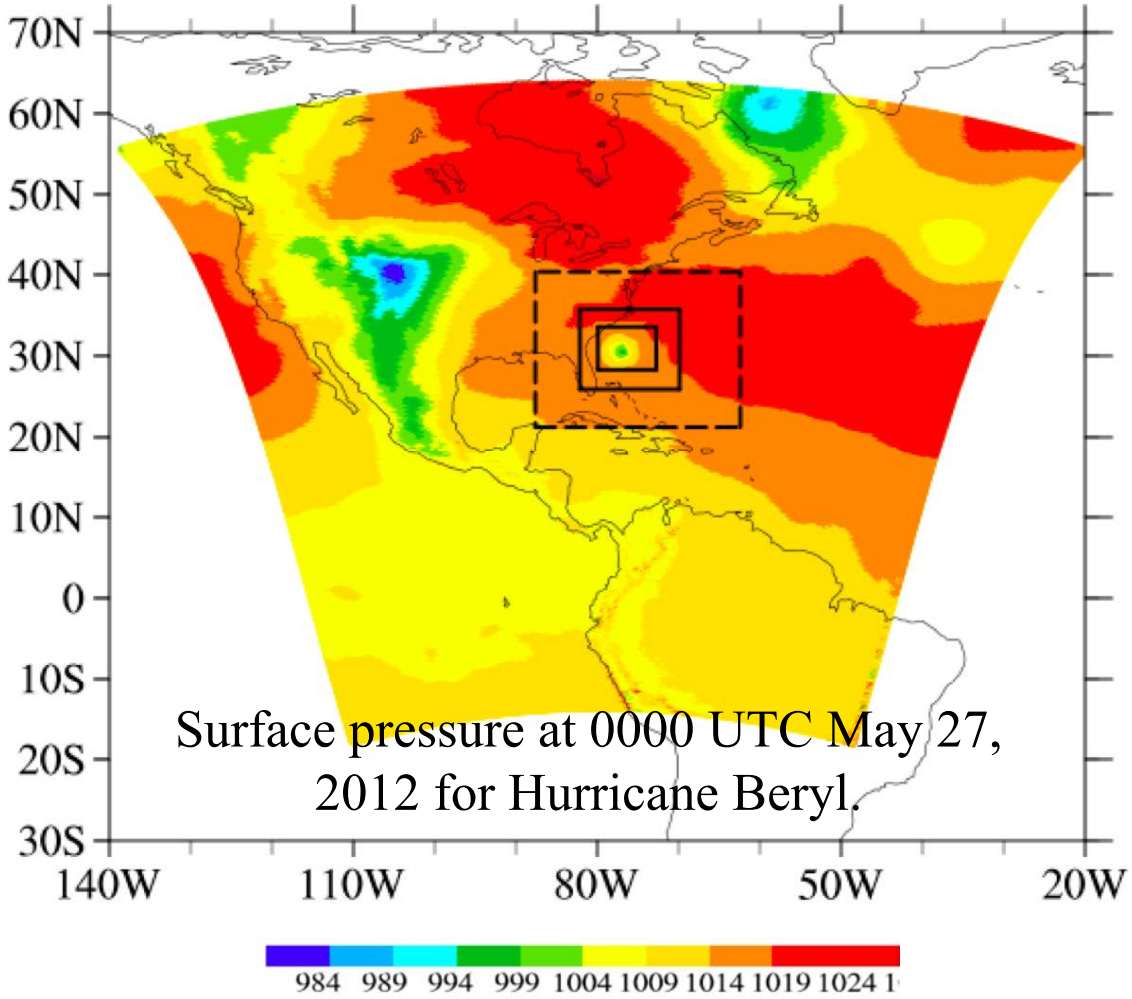

Surface pressure at 0000 UTC May 27, 2012 for Hurricane Beryl.

Four 2012 Atlantic Hurricanes which Made Landfall

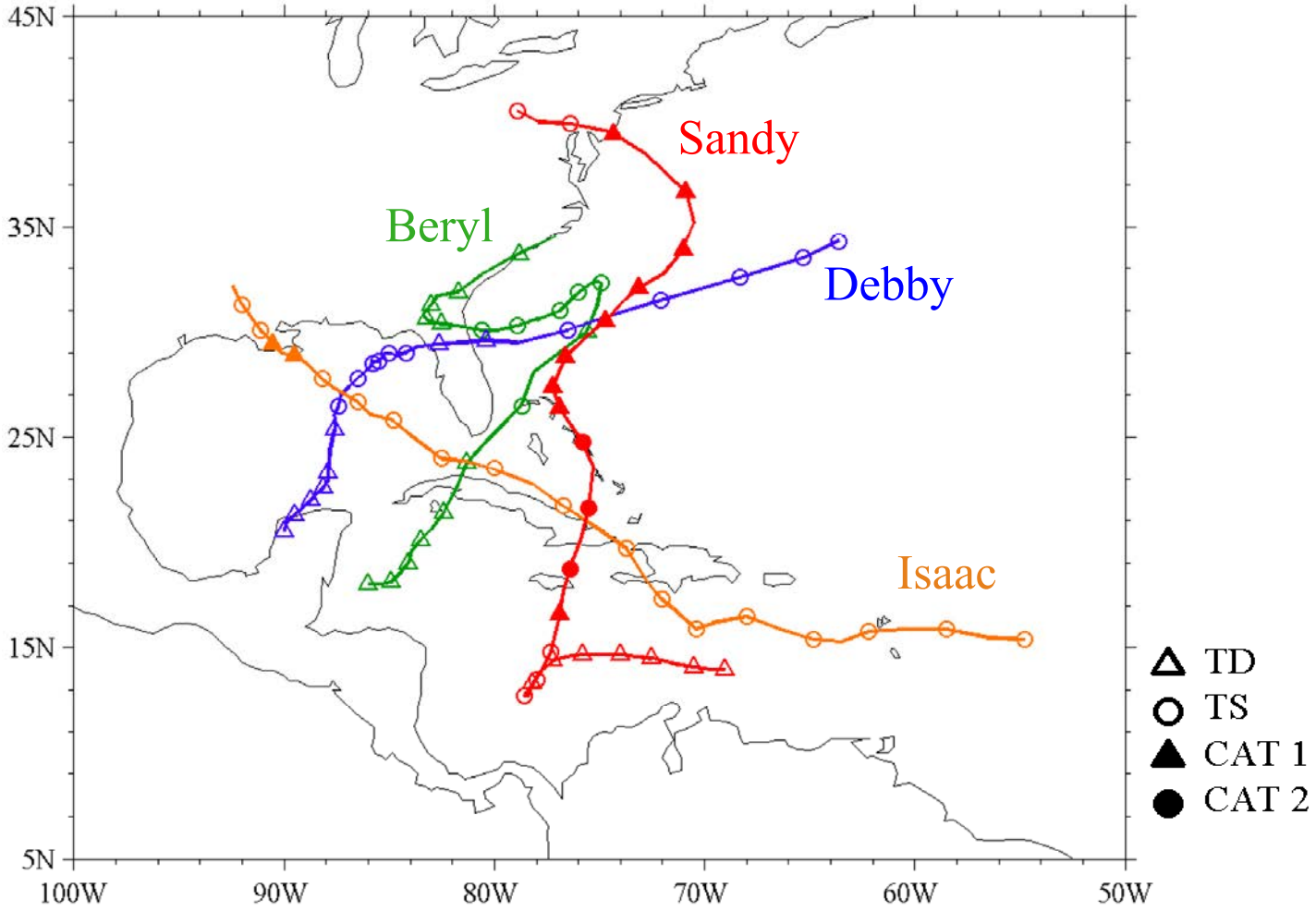

O-B Values for Those Data Points that Pass QC

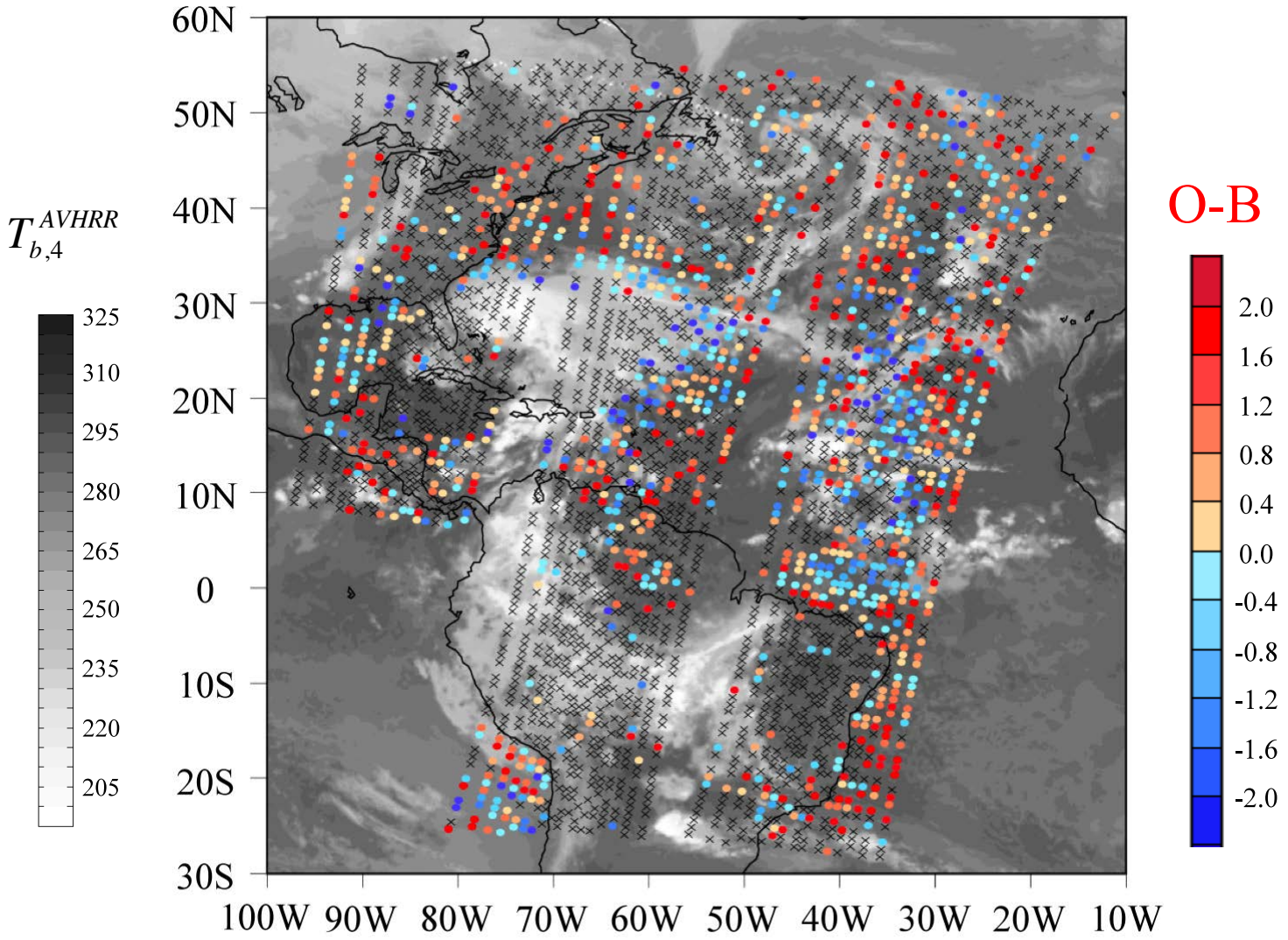

0600 UTC October 26, 2012

Data Points Removed by QC

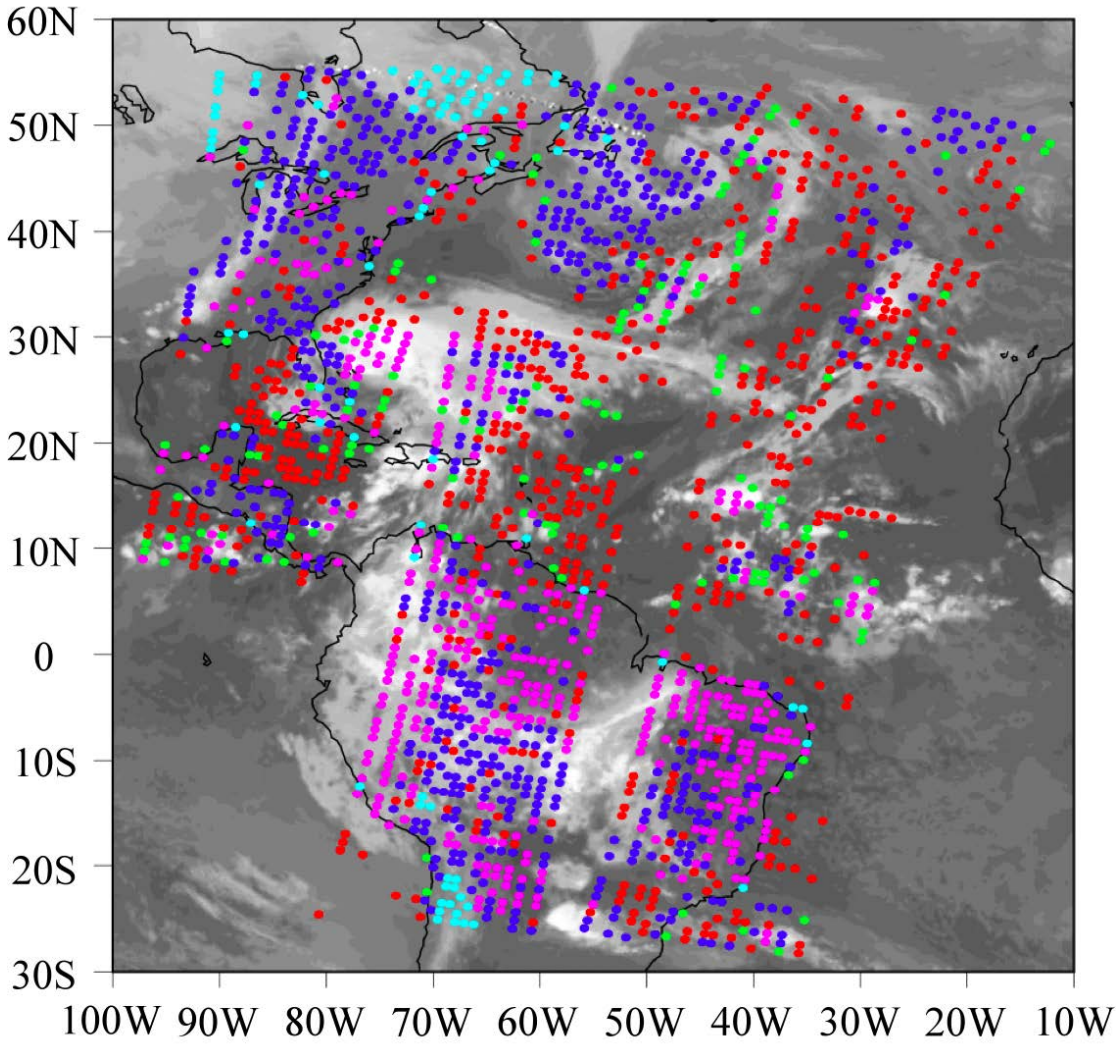

the 5th QC
the 6th QC
the 7th QC
the 8th QC
the 9th QC
criteria

0600 UTC October 26, 2012

Convergence of ATMS Data Assimilation (Isaac)

ATMS channel 6

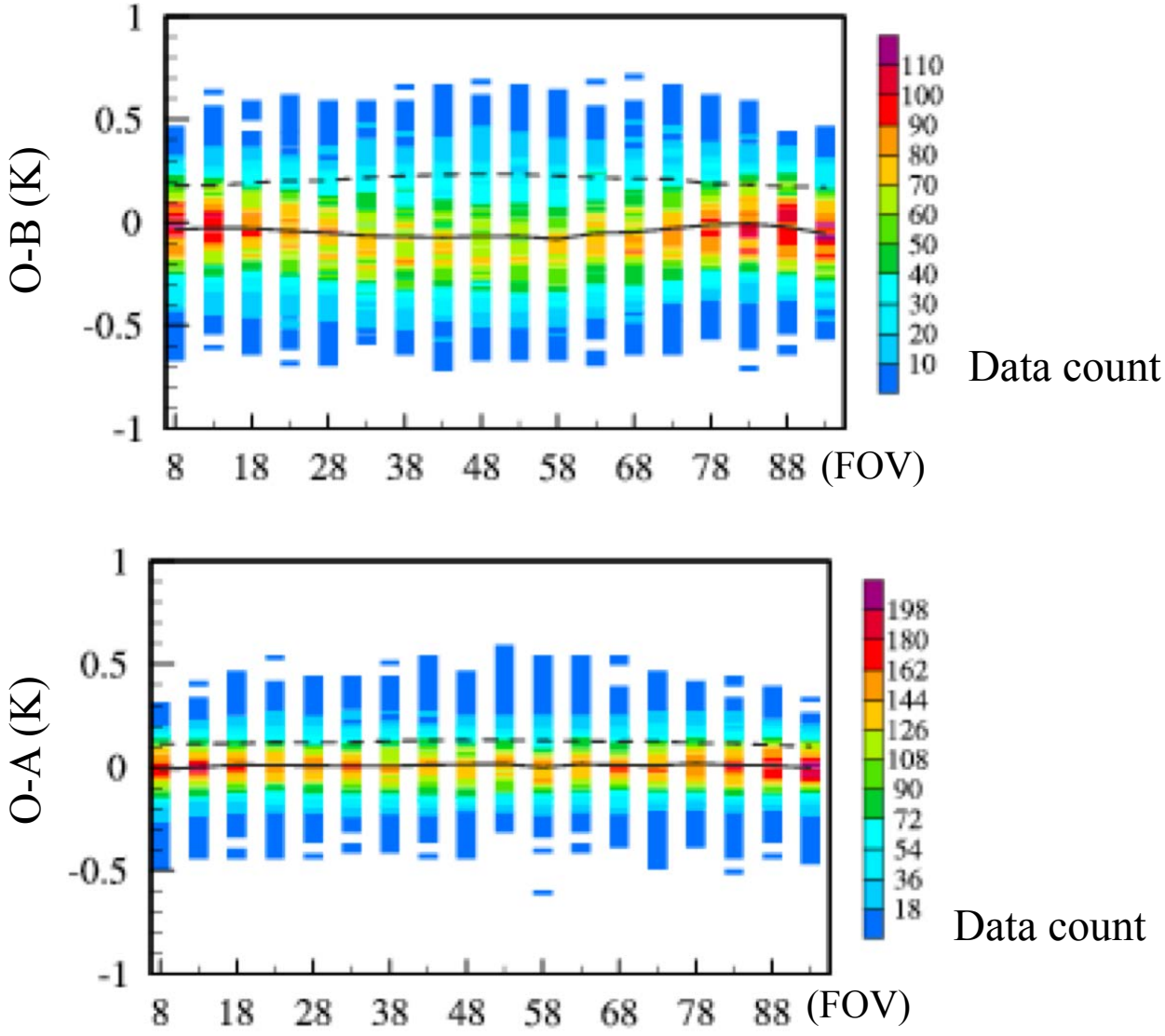

Convergence of ATMS Data Assimilation (Isaac)

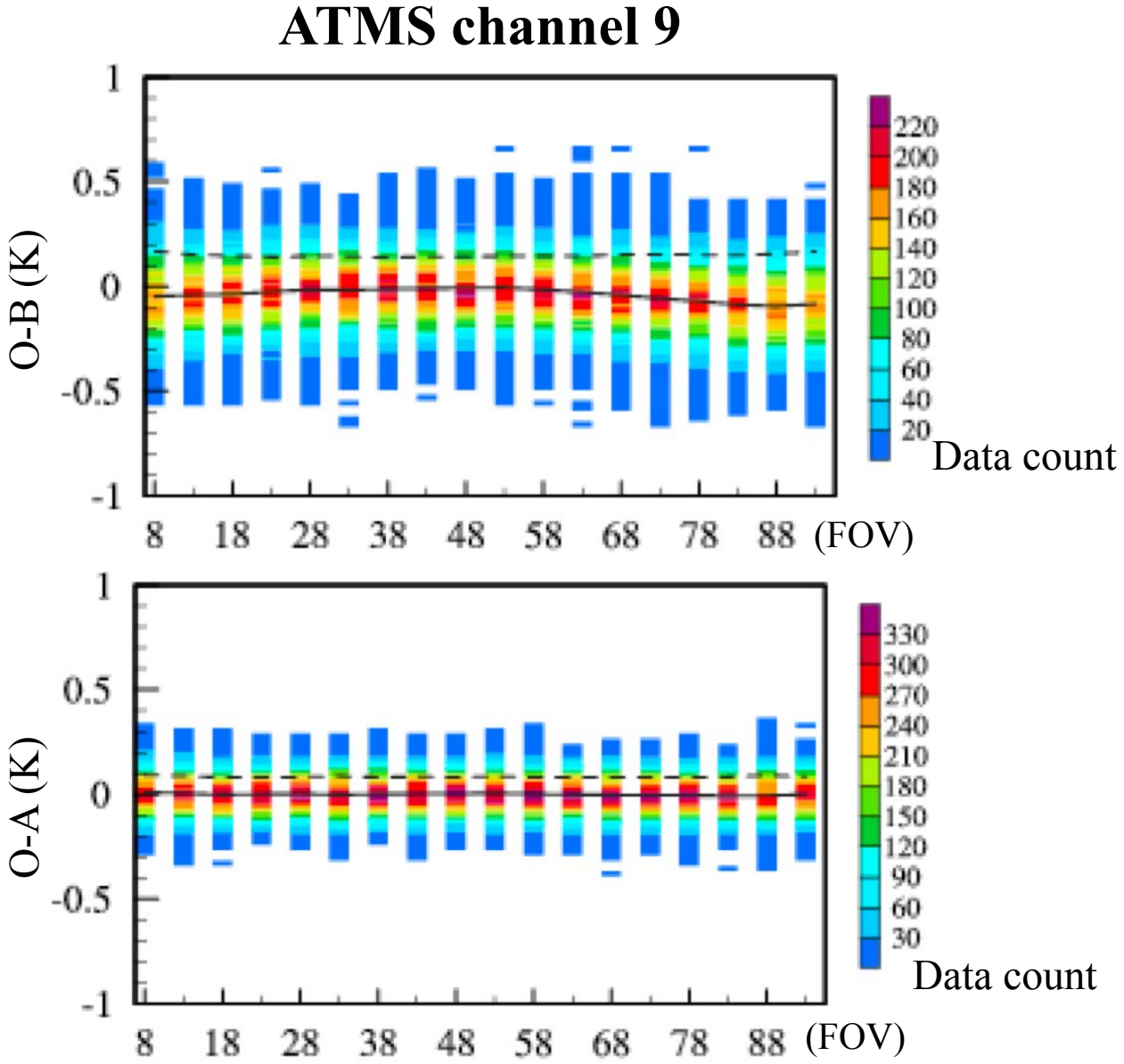

Standard Deviation before and after Data Assimilation For Hurricane Isaac

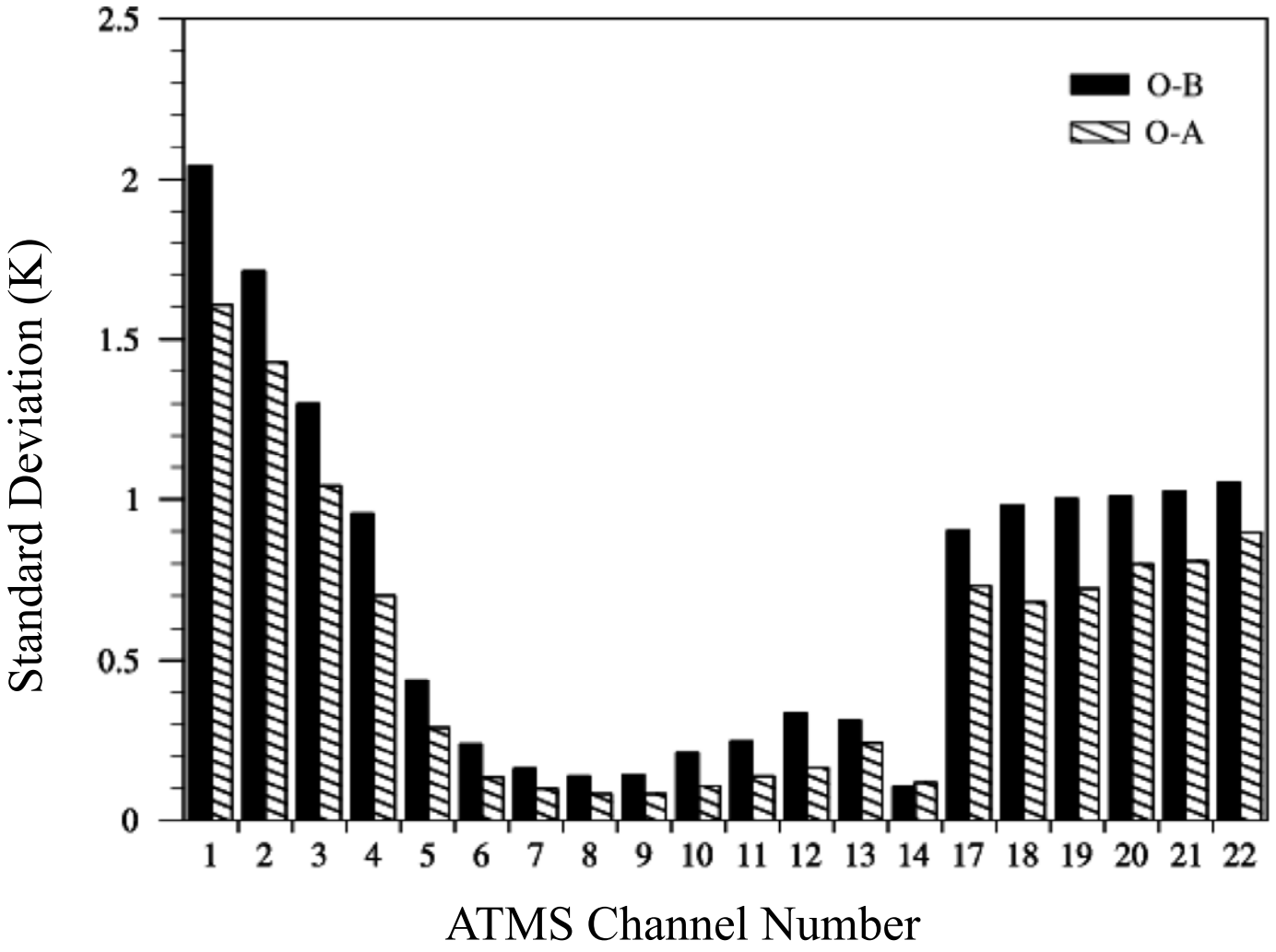

Daily Mean Forecast Errors For Isaac

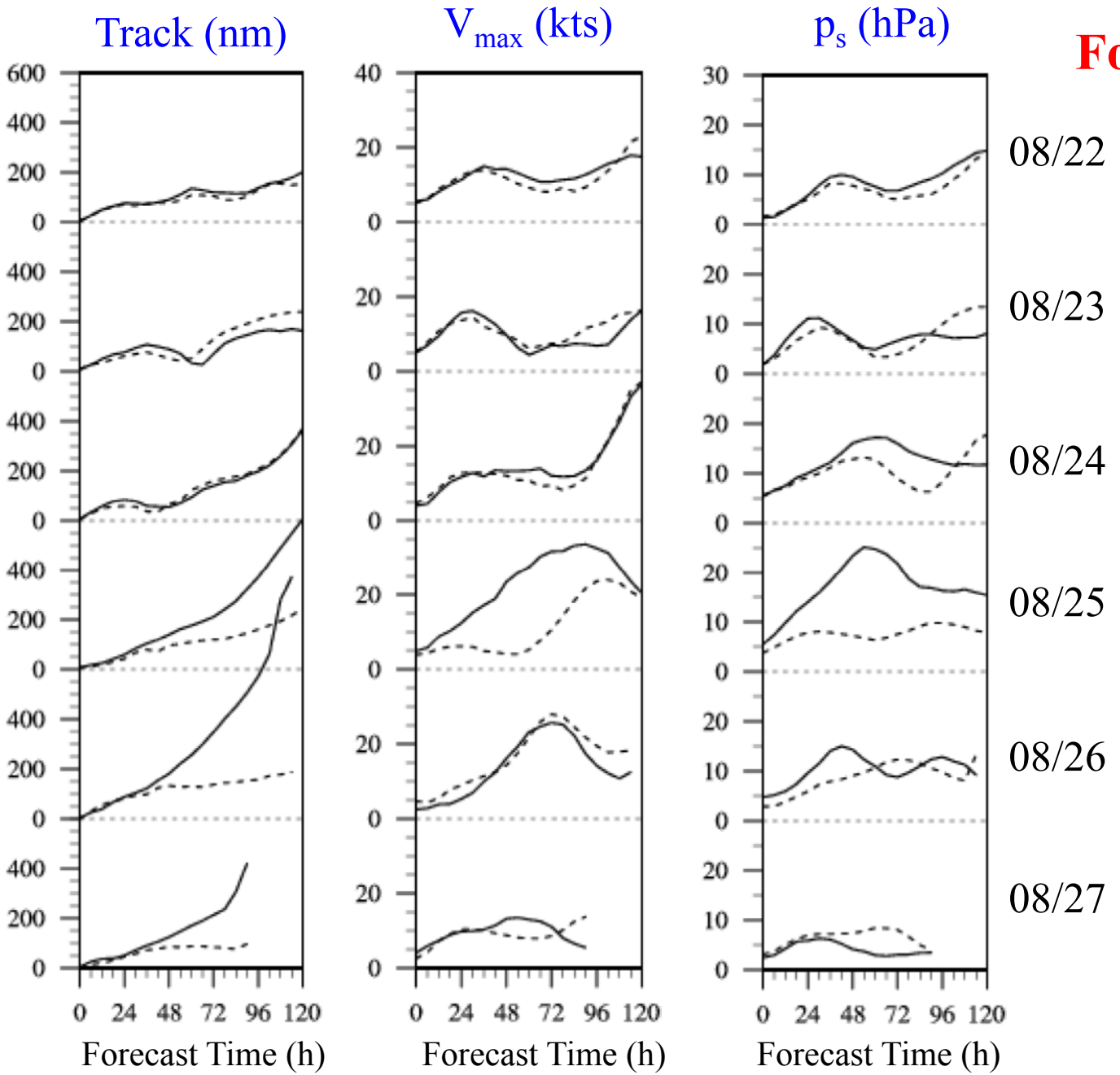

Impacts of Satellite Data Assimilation on v_{max} Forecast Errors for Hurricane Isaac

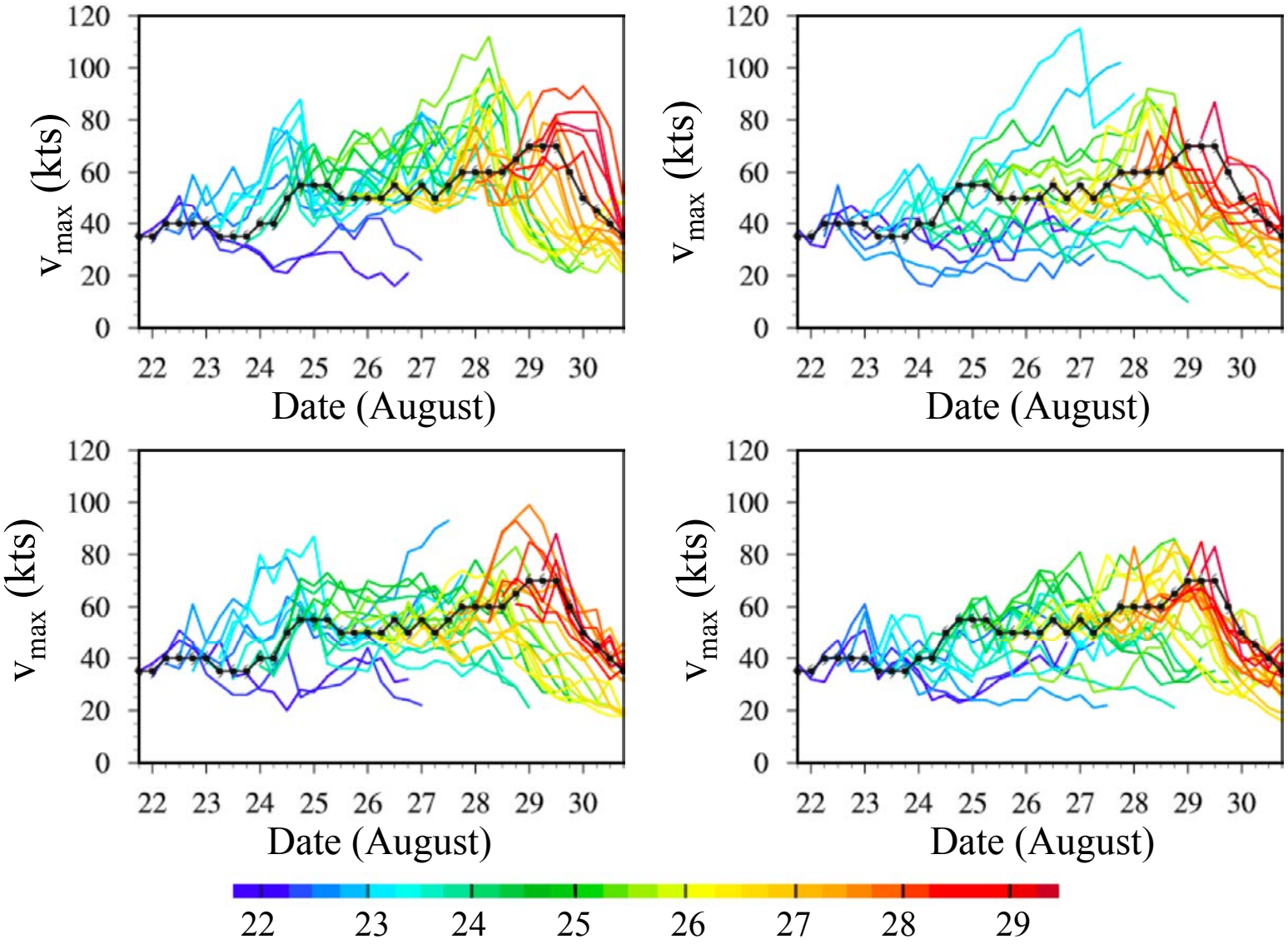

Impacts of ATMS Data Assimilation on the Track Forecast of Hurricane Sandy

without ATMS

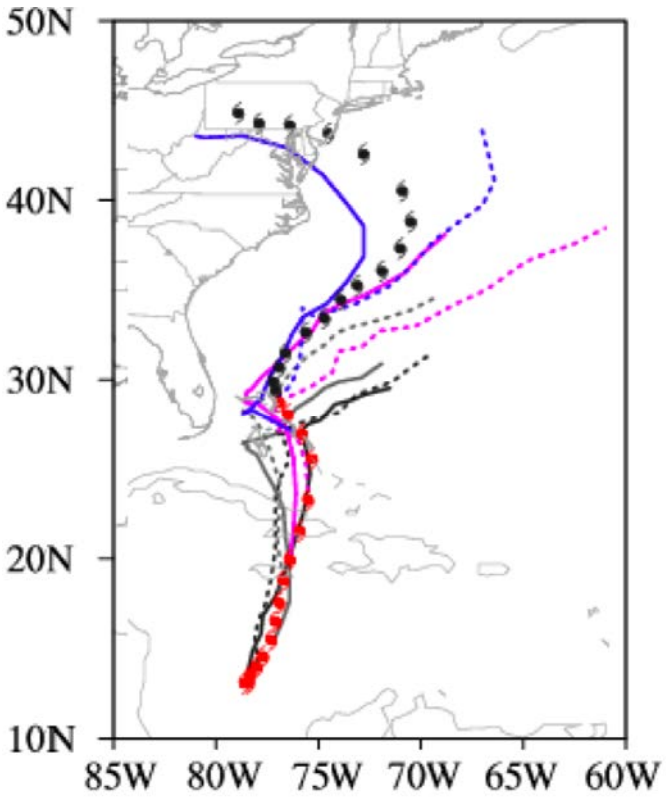

with ATMS

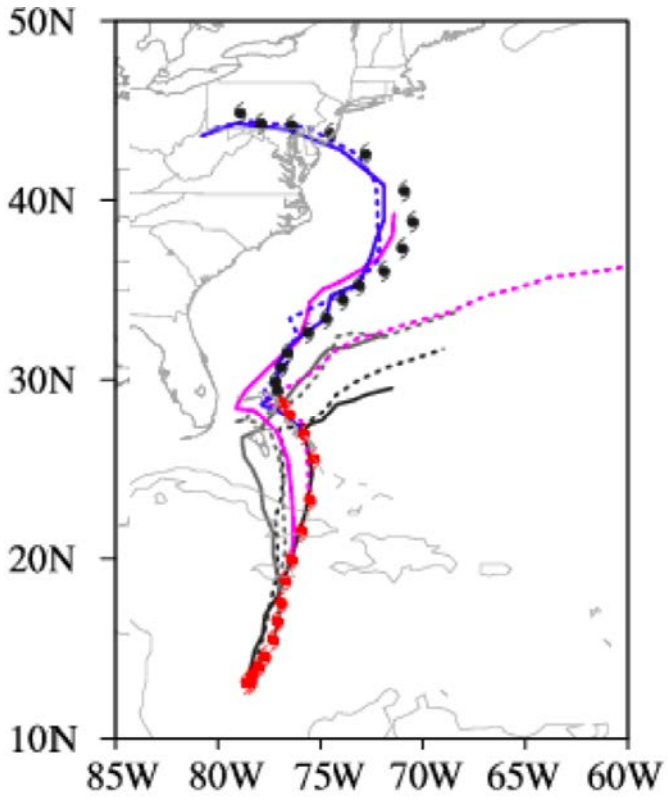

23 24 25 26 27 28 29 (October)

72-h Forecasts of PV and Wind Vector at 200 hPa

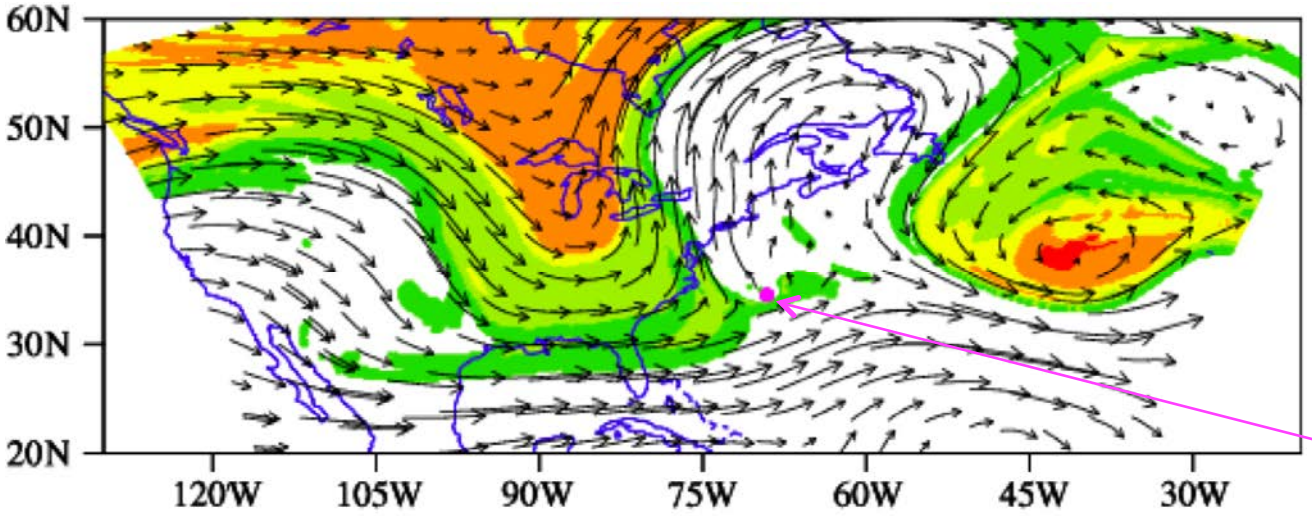

Without ATMS

Sandy

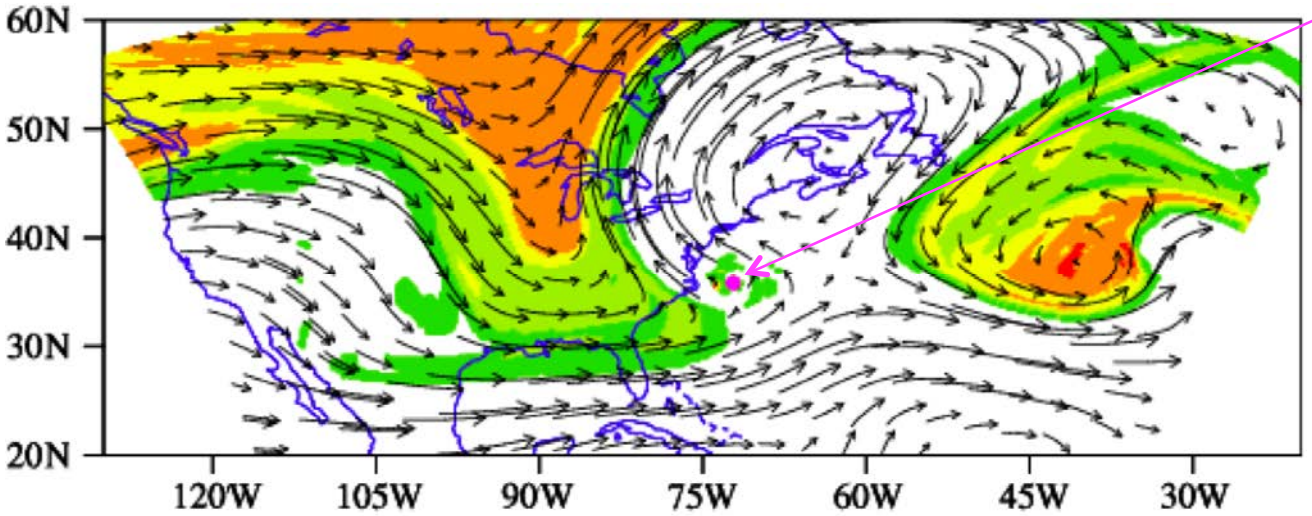

With ATMS

84-h Forecasts of PV and Wind Vector at 200 hPa

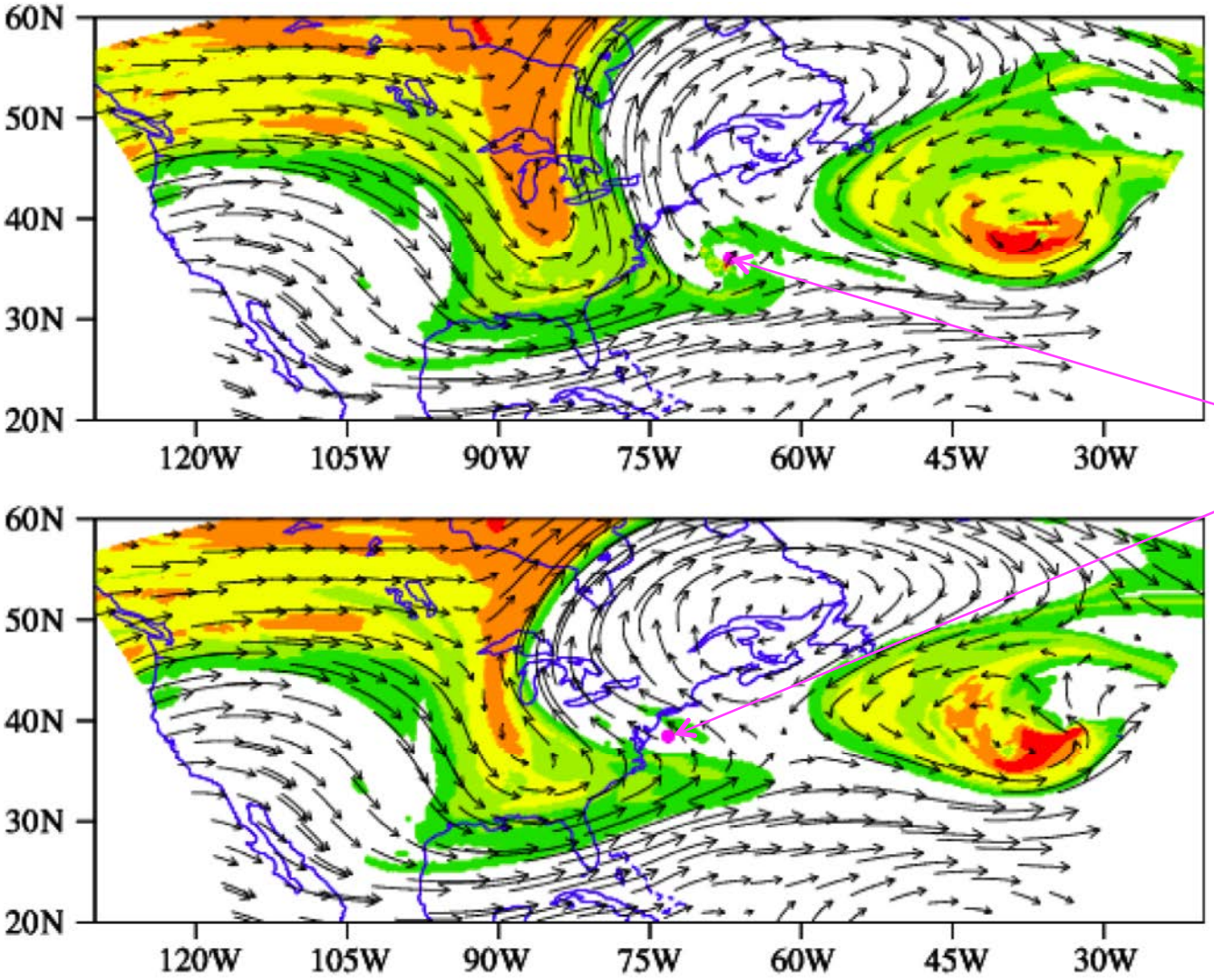

Without ATMS

Sandy

With ATMS

84-h Forecasts of Cloud Liquid Water Valid at 0000 UTC 30 October 2012

Without ATMS

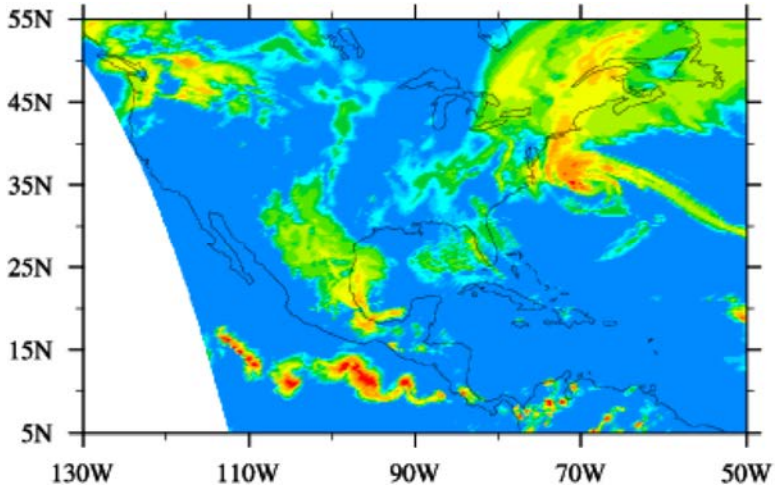

With ATMS

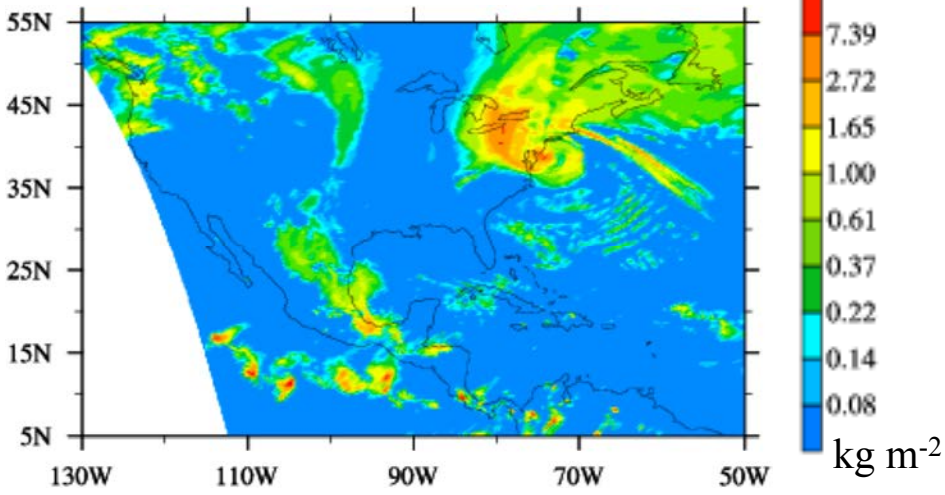

GOES-13 $T_{b,4}$ for Verification

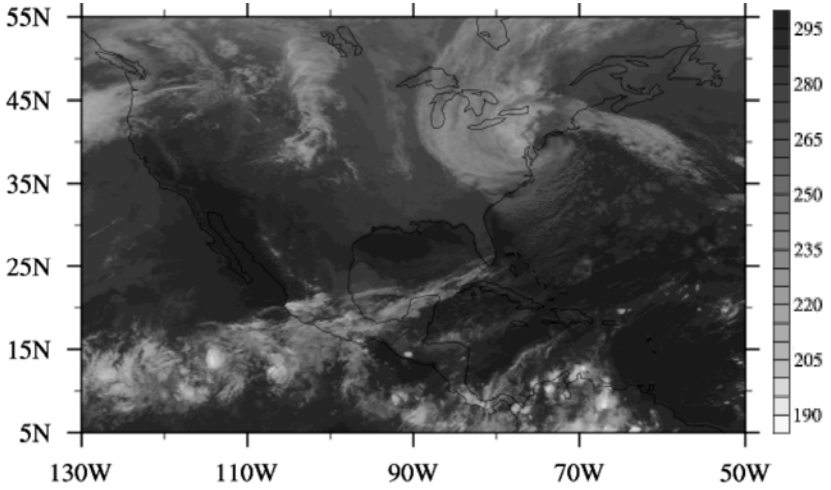

ATMS $T_{b,18}$ at 1727 UTC 10/29/12

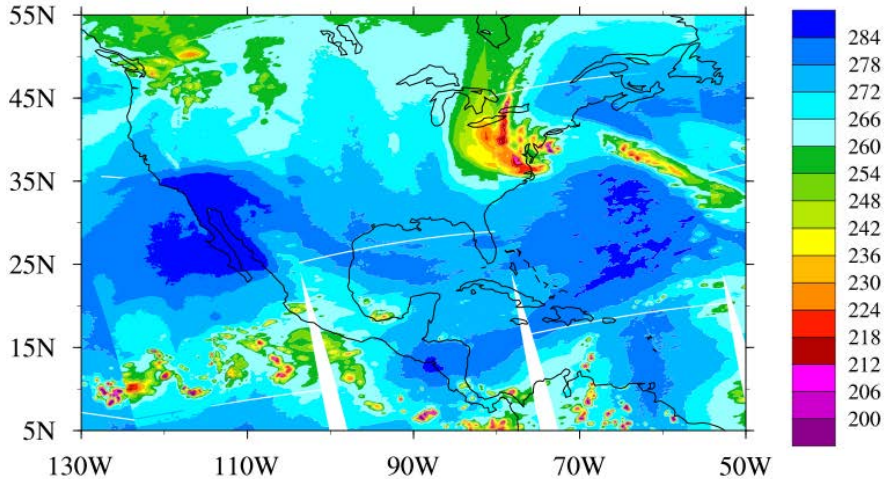

Mean Forecast Errors for 2012 Atlantic Landfalling

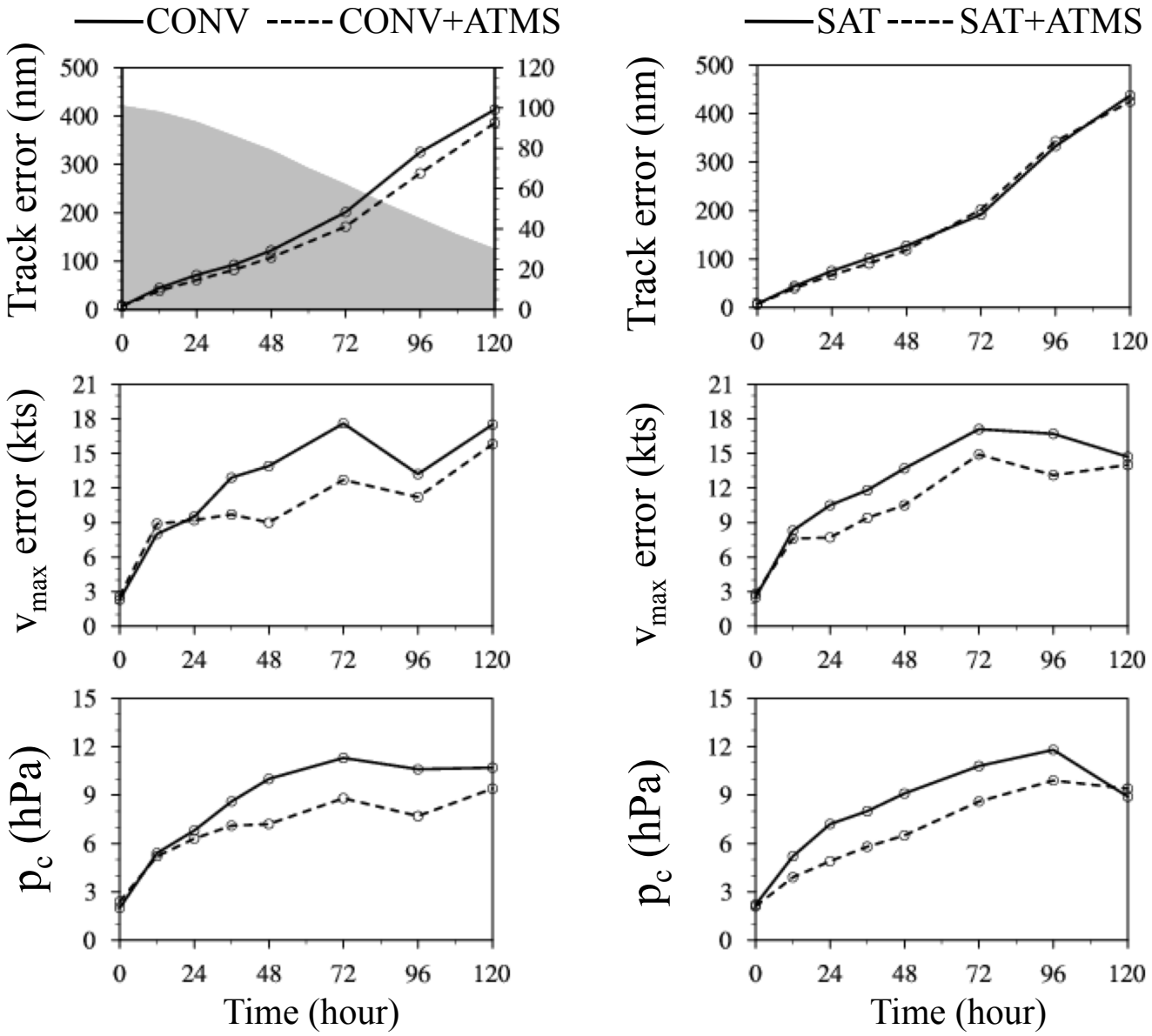

Summary (Part I)

- AMSU-A and GOES imager data contribute most significantly to improved QPFs near Gulf of Mexico
- Assimilation of GOES imager radiances contributes positively to any single type of satellite data
- Assimilation of all types of satellite data in the GSI system did not produce a better forecast than any experiment assimilated a single type of satellite data
- An improved cloud detection for MHS observations results in a significant positive impact to coastal QPFs

Summary (Part II)

- Some cloudy radiances remain near cloud edges after the MHS QC in GSI
- The cloud detection algorithm effectively removes those cloudy radiances remaining near cloud edges after the MHS QC in GSI
- The MHS data assimilation with the revised QC is shown to significantly improve coastal QPFs

Summary (Part III)

- A consistent FOV distribution between temperature and humidity channels on ATMS makes the cloud detection easy to implement

- ATMS data assimilation in GSI/HWRF results in a consistent positive impact on the track and intensity forecasts of the four landfall hurricanes in 2012

- Hurricane Sandy's forecasts are significantly improved after ATMS data assimilation when verified with independent GOES and POES observations

More details can be found in

Zou, X., Z. Qin, and F. Weng, 2012: Improved coastal precipitation forecasts with direct assimilation of GOES 11/12 imager radiances, *Mon. Wea. Rev.*, **139**, 3711-3729.

Qin, Z., X., Zou, and F. Weng, 2013: Evaluating added benefits of assimilating GOES imager radiance data in GSI for coastal QPFs. *Mon. Wea. Rev.*, **141**(1), 75-92.

Zou, X., Z. Qin, and F. Weng, 2013: Improved quantitative precipitation forecasts by MHS radiance data assimilation with a newly added cloud detection algorithm, *Mon. Wea. Rev.*, **141**, 3203-3221.

Weng, F., X. Zou, X. Wang, S. Yang, and M. D. Goldberg, 2012: Introduction to Suomi NPP ATMS for NWP and tropical cyclone applications. *J. Geophy. Res.*, **117**, D19112, 14pp, doi:10.1029/2012JD018144.

Zou, X., F. Weng, B. Zhang, L. Lin, Z. Qin and V. Tallapragada, 2013: Impact of ATMS radiance data assimilation on hurricane track and intensity forecasts using HWRF. *J. Geophy. Res.* JPSS Special Issue, (revised)

Acknowledgement

This work was supported by NOAA GOES-R risk reduction program and JPSS Proving Ground Program.